On Spurious Numerics in Solving Reactive Equations

Fractional Step vs. Fully Coupled Procedures

(Problems Containing Stiff Source Terms & Discontinuities)

H.C. Yee, NASA Ames Research Center

(Joint work: D. Kotov, W. Wang, C.-W. Shu & B. Sjogreen)

JRV Symposium - CFD: Looking Back & Moving Forward, June 22-23, 2013, San Diego

Outline

- **Goal:** *Gain a deeper understanding of spurious behavior of shock-capturing schemes -- different procedures in solving the reactive Eqns.*

  > *Strang splitting + with or without safeguard procedure*
  > *(Ad hoc method to include a cut off safeguard procedure if density is outside the permissible range)*

  > *Fully coupled system + with or without safeguard procedure (No-Strang)*

- **Numerical Methods with Dissipation Control**
  > *Turbulence with strong shocks & stiff source terms*
  > *Can delay the onset of wrong speed for stiffer problems*

- **1D & 2D Test Cases with 2 & 13 Species**

- **Conclusions & Future Plan**

Spurious Behavior: Wrong propagation speed of discontinuities

Wrong Propagation Speed of Discontinuities

(Standard Shock-Capturing Schemes: TVD, WENO5, WENO7)

Chapman-Jouguet (C-J)
1D detonation wave,
e.g. *Helzel et al. 1999*

Arrhenius Reaction Rate:

$$K(T) = K_0 \exp\left(\frac{-T_{ign}}{T}\right)$$

K_0 can be large
(stiff coeff.)

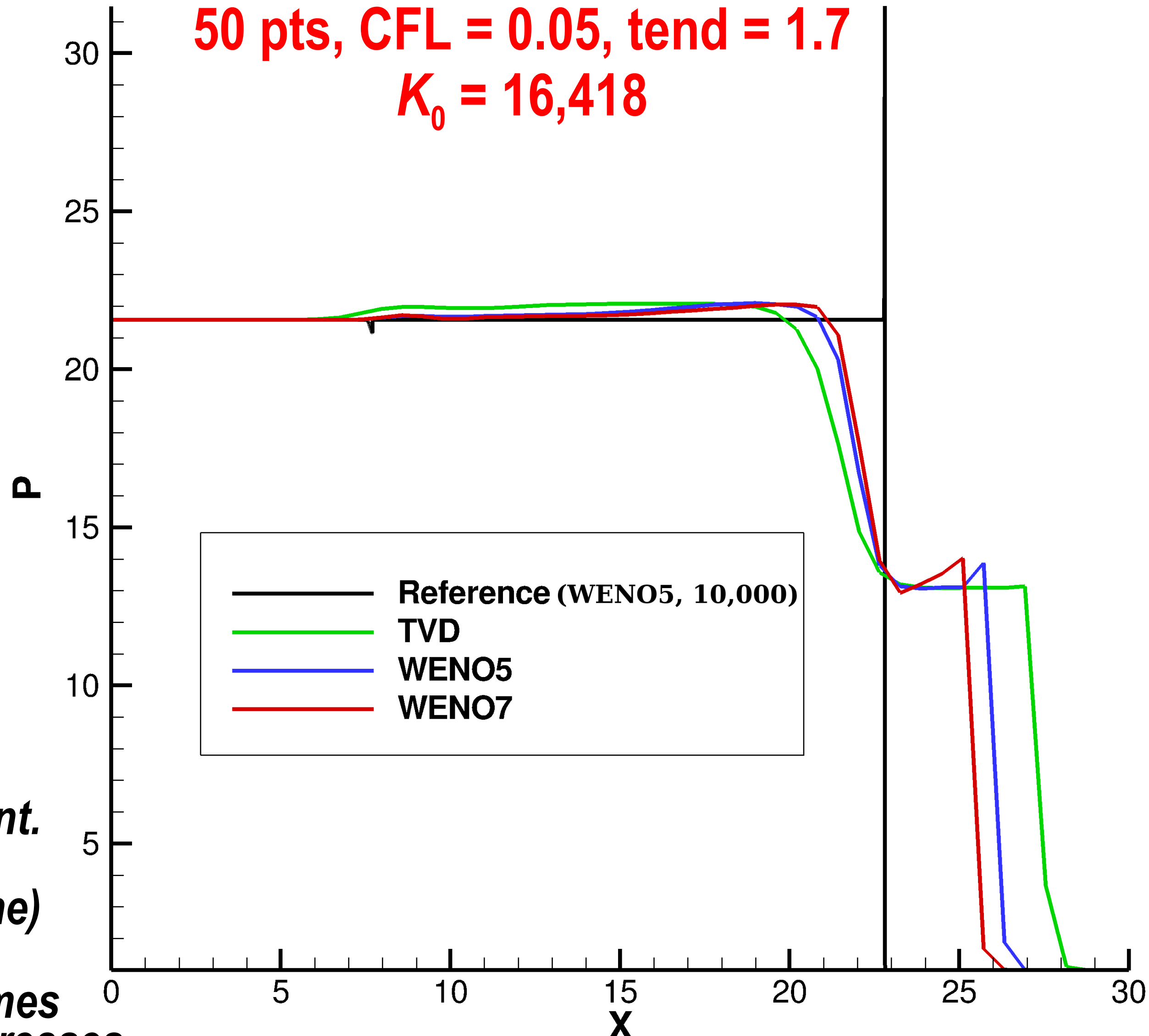

Notes:

- *Concern capturing the correct discont. location with coarse grid (not address the narrow reaction zone)*
- *The wrong propagation speed becomes more pronounced as stiffness K_0 increases*

Strang Splitting & Safeguard

High Order Methods with Subcell Resolution

(Wang, Shu, Yee & Sjögreen, JCP, 2012)

Procedure:

Split equations into convective and reactive operators
(Strang-splitting 1968)

$$U_t + F(U)_x + G(U)_y = S(U)$$

$$U_t + F(U)_x + G(U)_y = 0 \qquad\qquad \frac{dU}{dt} = S(U)$$

A – Convection operator

R – Reaction operator
(RK1, RK2, RK3, RK4)

Numerical solution: $$U^{n+1} = A\left(\frac{\Delta t}{2}\right) R(\Delta t)\, A\left(\frac{\Delta t}{2}\right) U^n$$

or: $$U^{n+1} = A\left(\frac{\Delta t}{2}\right) R\left(\frac{\Delta t}{N_r}\right) \ldots R\left(\frac{\Delta t}{N_r}\right) A\left(\frac{\Delta t}{2}\right) U^n$$

N_r – Number of subiterations

Subcell Resolution (SR) Method Basic Approach

- Any high resolution shock capturing method can be used in the convection step

  Test case: WENO5 with Roe flux & RK4

- Any standard shock-capturing scheme produces a few transition points in the shock

  => Solutions from the convection step, if applied directly to the reaction step, result in wrong shock speed

New Approach: Apply Subcell Resolution (Harten 1989; Shu & Osher 1989) to the solution from the convection operator step before the reaction step

Note: if $N_r > 1$ apply SR at each subiteration

Well-Balanced High Order Filter Schemes for Reacting Flows *(Any number of species & reactions)*

Yee & Sjögreen, 1999-2010, Wang et al., 2009-2010

Preprocessing step

Condition (equivalent form) the governing equations by, e.g., Ducros et al. Splitting (2000) to improve numerical stability

High order base scheme step (Full time step)

- 6^{th}-order (or higher) central spatial scheme & 3^{rd} or 4^{th}-order RK
- SBP numerical boundary closure, matching order conservative metric eval.

Nonlinear filter step

- Filter the base scheme step solution by a dissipative portion of high-order shock capturing scheme, e.g., WENO of 5^{th}-order
- Use Wavelet-based flow sensor to control the amount & location of the nonlinear numerical dissipation to be employed

Well balanced scheme: preserve certain non-trivial physical steady state solutions exactly

1D C-J Detonation Wave

(Helzel et al. 1999; Tosatto & Vigevano 2008)

Left state (totally burned gas)

Right state (totally unburned gas)

$$\begin{pmatrix} \rho_b \\ u_b \\ p_b \end{pmatrix} = \begin{pmatrix} \rho_u \dfrac{[p_b(\gamma+1)-p_u]}{\gamma p_b} \\ S_{CJ} - (\gamma p_b/\rho_b)^{1/2} \\ -b + (b^2 - c)^{1/2} \end{pmatrix}$$

$$\begin{pmatrix} \rho_u \\ u_u \\ p_u \end{pmatrix} = \begin{pmatrix} 1 \\ 0 \\ 1 \end{pmatrix}$$

$$S_{CJ} = [\rho_u u_u + (\gamma p_b \rho_b)^{1/2}]/\rho_u$$

$$b = -p_u - \rho_u q_0 (\gamma - 1) \qquad c = p_u^2 + 2(\gamma-1) p_u \rho_u q_0/(\gamma+1)$$

Ignition temperature $T_{ign} = 25$

Heat release $q_0 = 25$

Rate parameter $K_0 = 16418$

$$K(T) = K_0 \exp\left(\frac{-T_{ign}}{T}\right)$$

1D C-J Detonation (K_0 = 16418, 50 pts)

tend = 1.7

Temperature

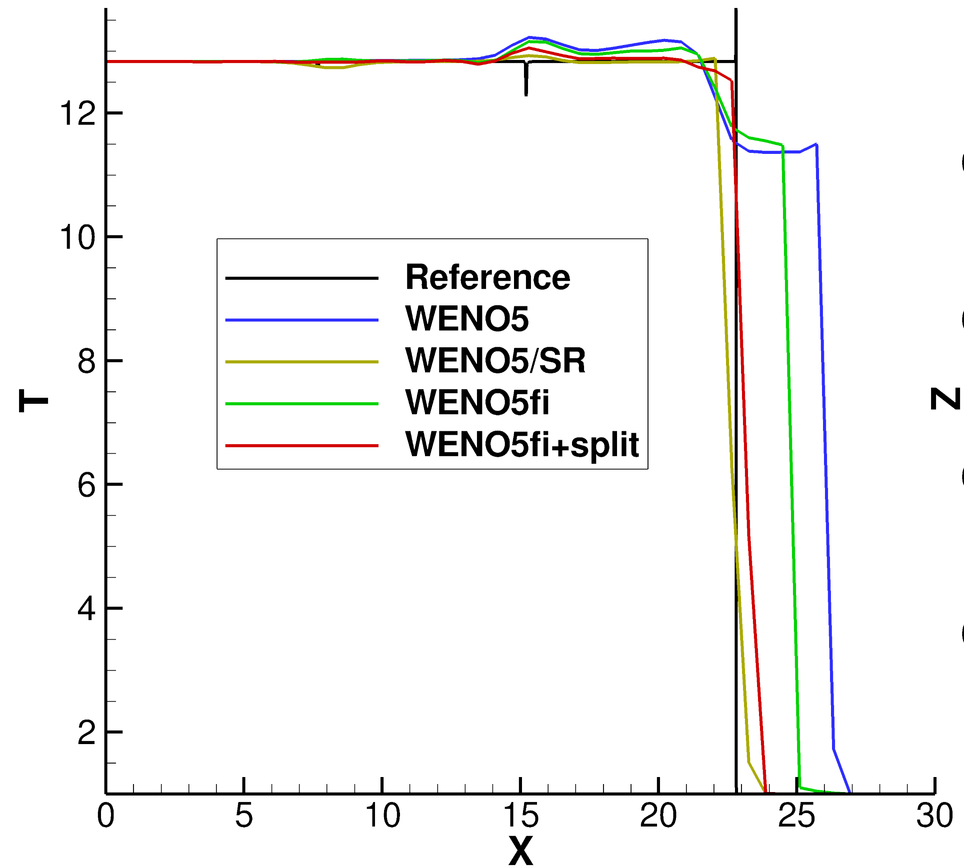

Mass Fraction

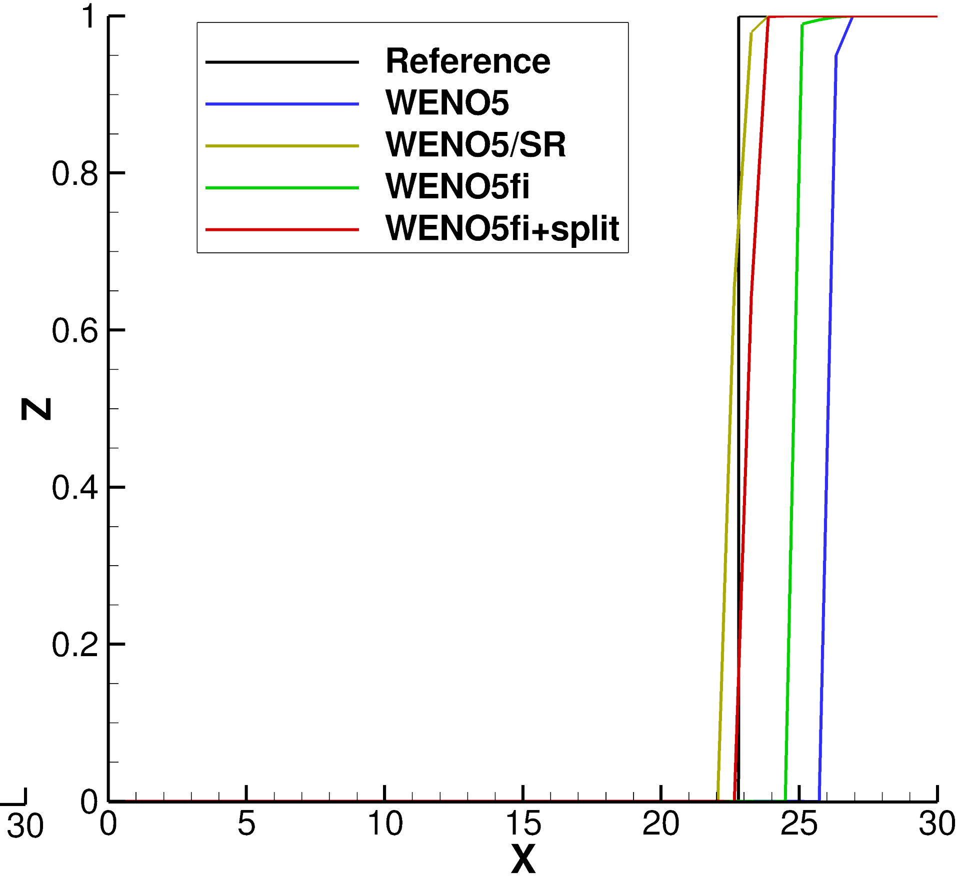

Standard Meth. – WENO5: Standard 5th order WENO (WENO7, TVD)

Improved Meth. –
- WENO5/SR: WENO5 + subcell resolution
- WENO5fi: filter version of WENO5
- WENO5fi+split: WENO5fi + preprocessing (Ducros splitting)

Reference: WENO5, 10,000 points

(Strang Splitting & Safeguard)

Behavior of the schemes below CFL limit

(Allowable Δt below CFL limit, consists of disjoint segments)

Strang Splitting & Safeguard, 50 pts, 100 K_0

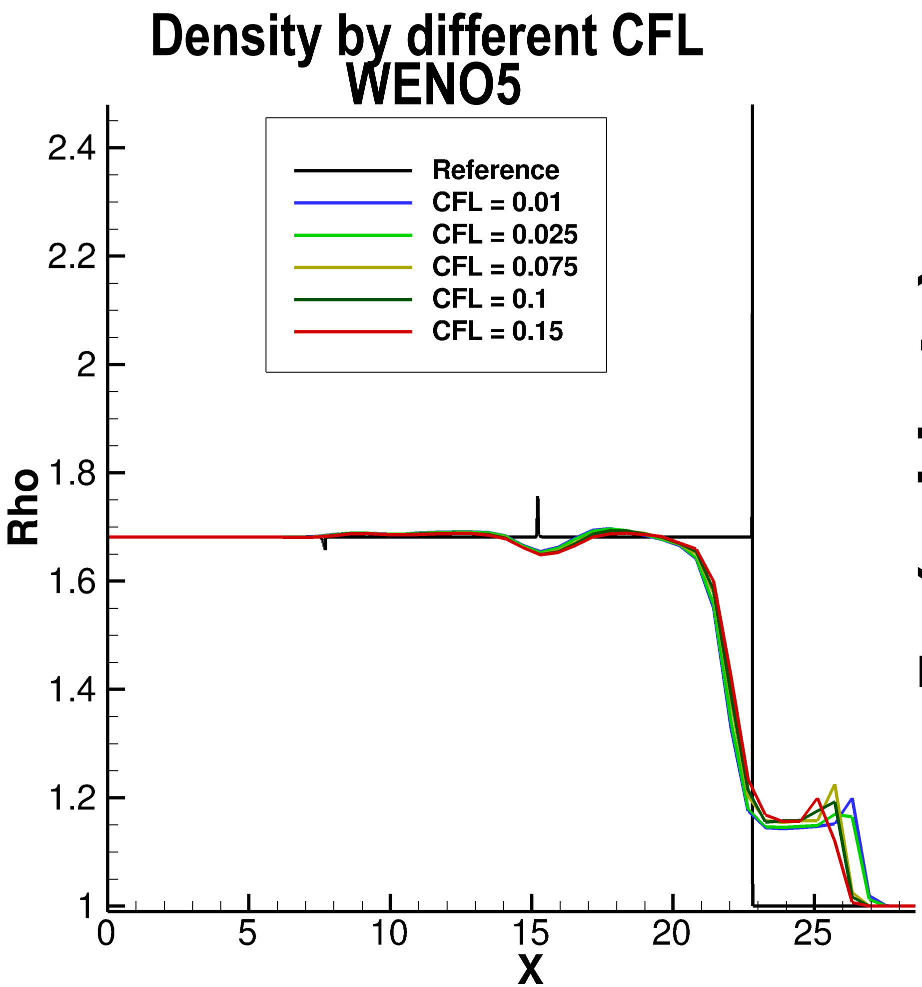

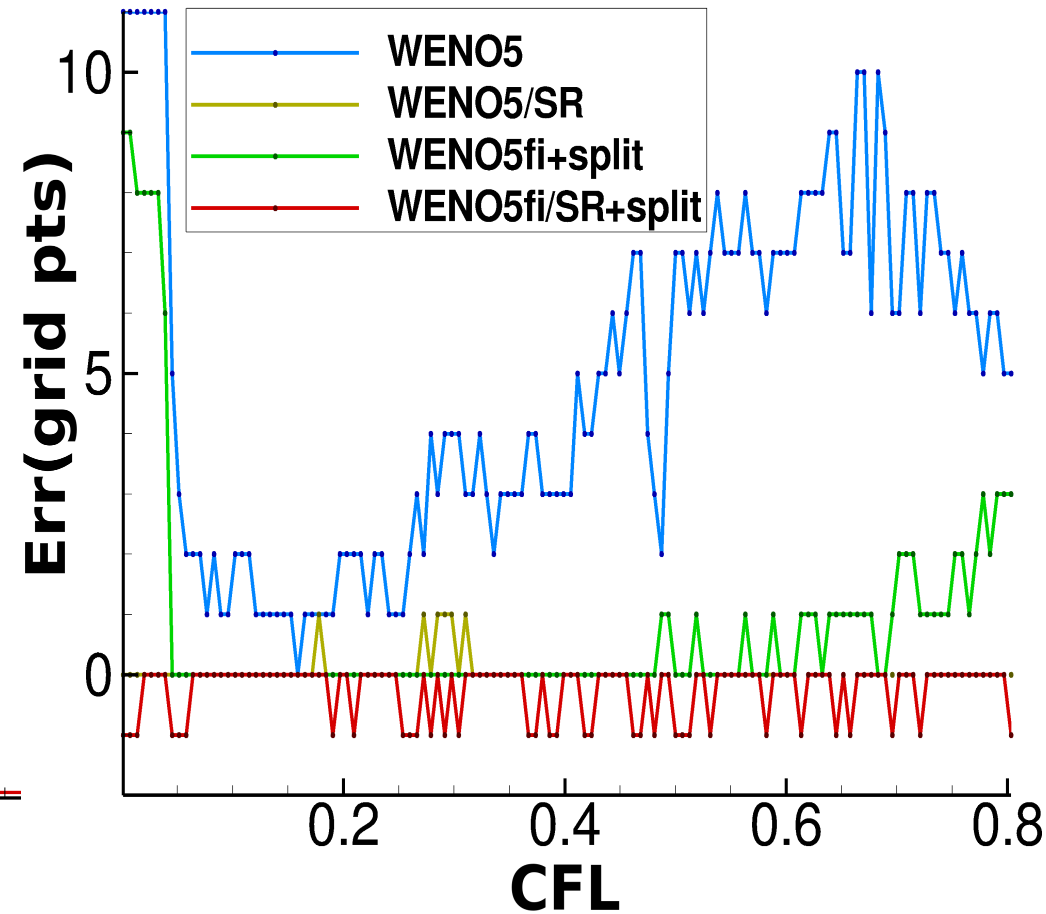

- *Incorrect or diverged solution may occur for Δt below CFL limit.*
- *CFL limit based on the convection part of PDEs*
- *Confirms the study by Lafon & Yee and Yee et al. (1990 - 2000)*

Behavior of Standard Schemes Below CFL Limit

(Strang vs. No-Strang: Safeguard; TVD, WENO5, WENO7)

1D C-J Detonation

Grid 50 **Grid 150** **Grid 300**

Strang/Safeguard

No-Strang/Safeguard

(Stable for small CFL)

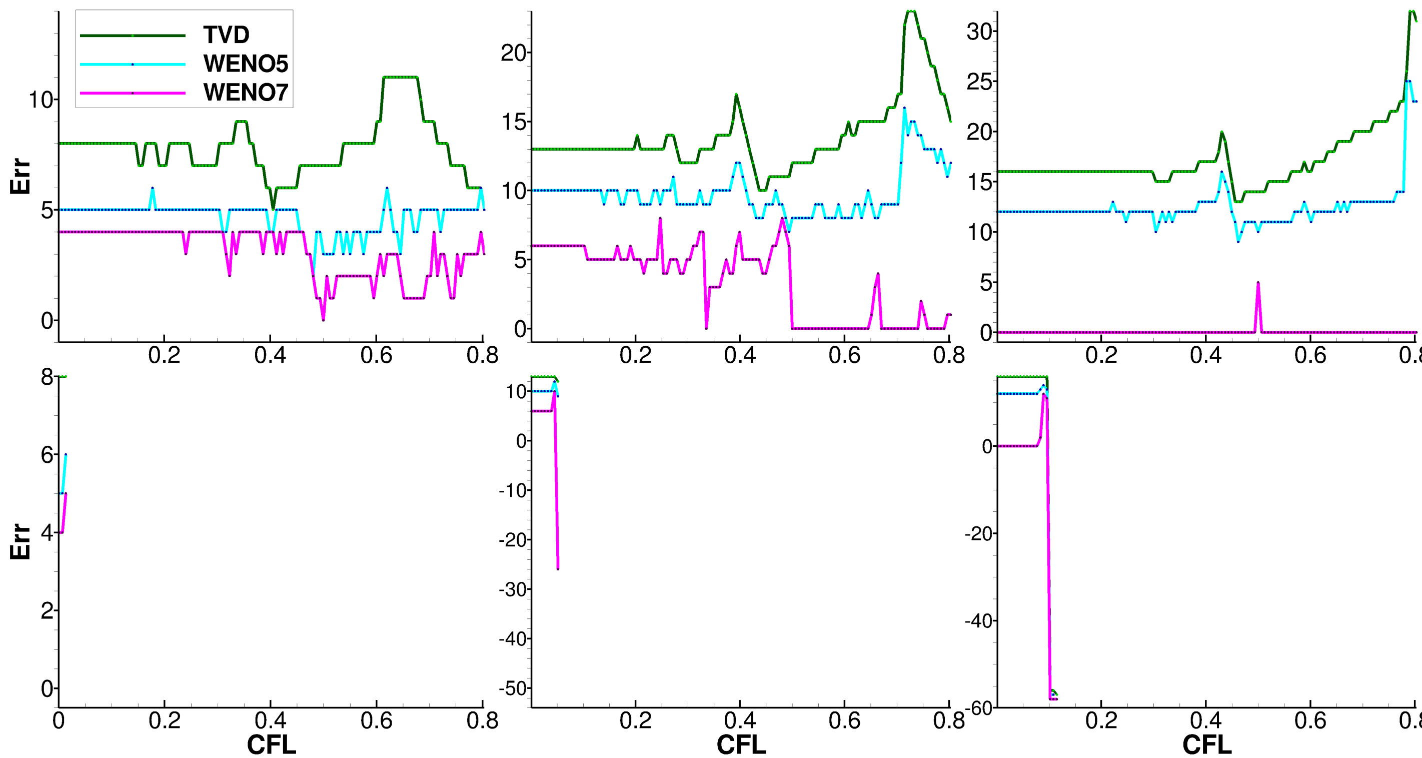

Err: # grid pts. away from exact shock location

Note: Among the 3 standard schemes, WENO7 exhibits the least spurious behavior as grid increases

Behavior of Standard Schemes Below CFL Limit
(Strang vs. No-Strang: No Safeguard; TVD, WENO5, WENO7)

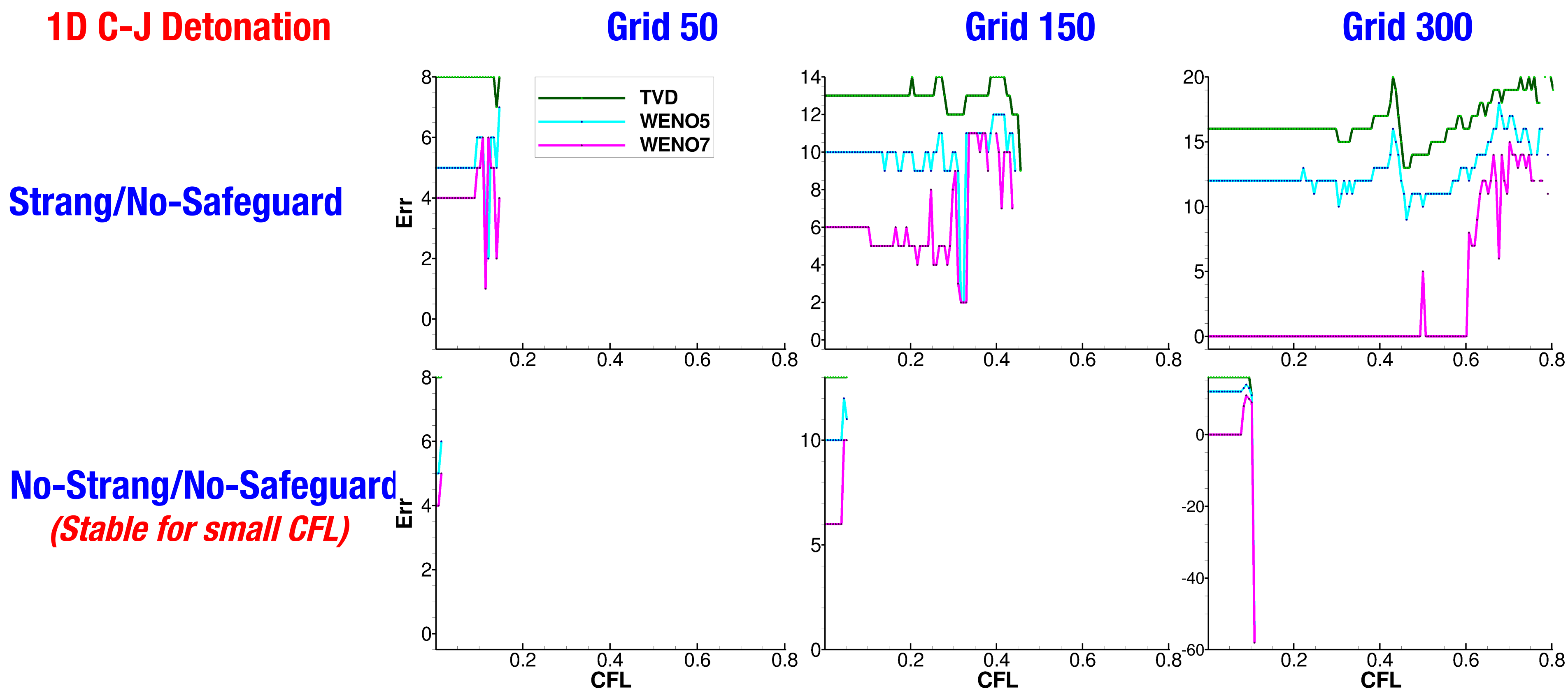

Err: # grid pts. away from exact shock location

Note: Among the 3 standard schemes, WENO7 exhibits the least spurious behavior as grid increases

Behavior of Improved Schemes Below CFL Limit

(Strang vs. No-Strang: Safeguard; WENO5/SR, WENO5fi, WENO5fi+split)

1D C-J Detonation

Grid 50 **Grid 150** **Grid 300**

Strang/Safeguard

No-Strang/Safeguard

(Stable for small CFL)

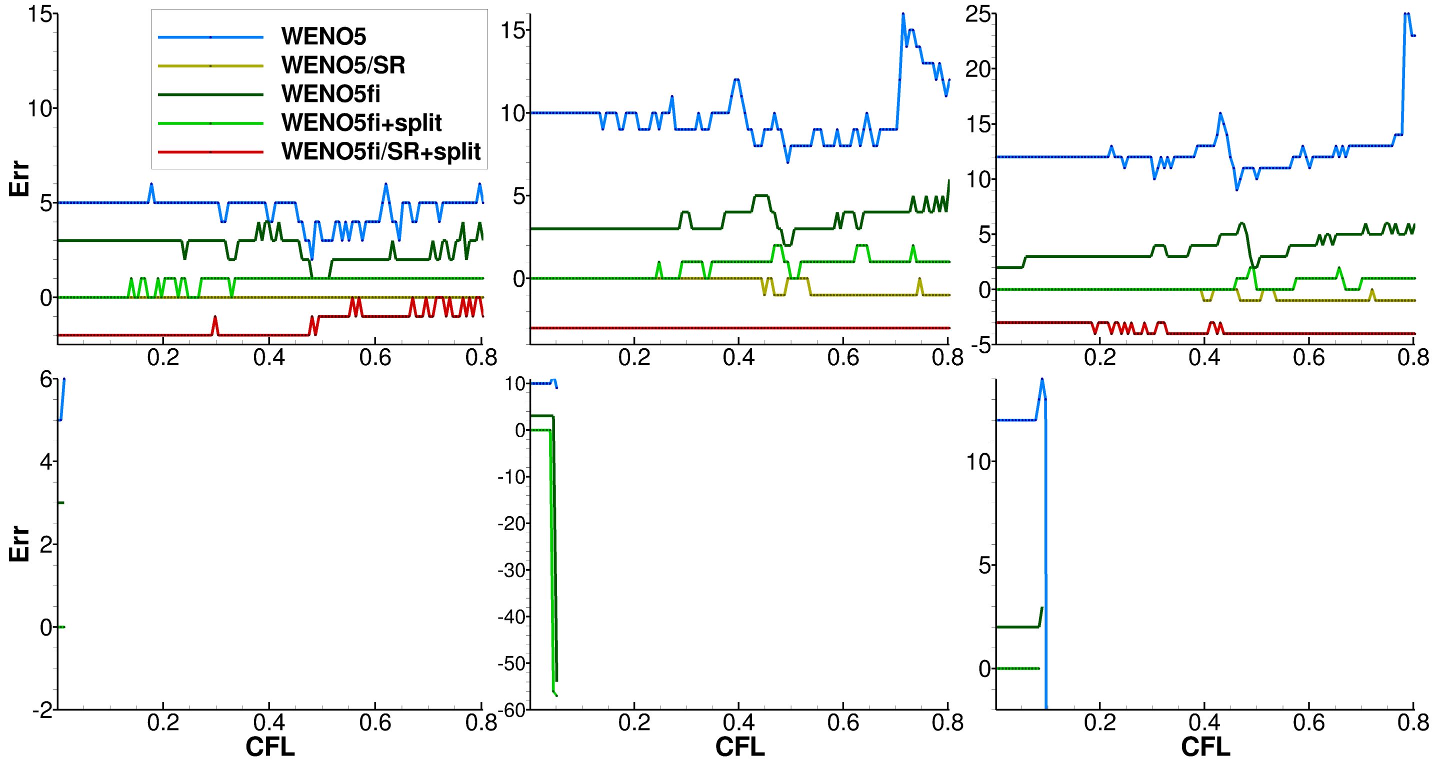

Err: # grid pts. away from exact shock locations

Note: *Among the 4 improved schemes **WENO5/SR & WENO5fi+split** exhibit the least spurious behavior as grid increases*

Behavior of Improved Schemes Below CFL Limit

(Strang vs. No-Strang: No Safeguard;   WENO5/SR, WENO5fi, WENO5fi+split)

1D C-J Detonation **Grid 50** **Grid 150** **Grid 300**

Strang/No-Safeguard

No-Strang/No-Safeguard
(Stable for small CFL)

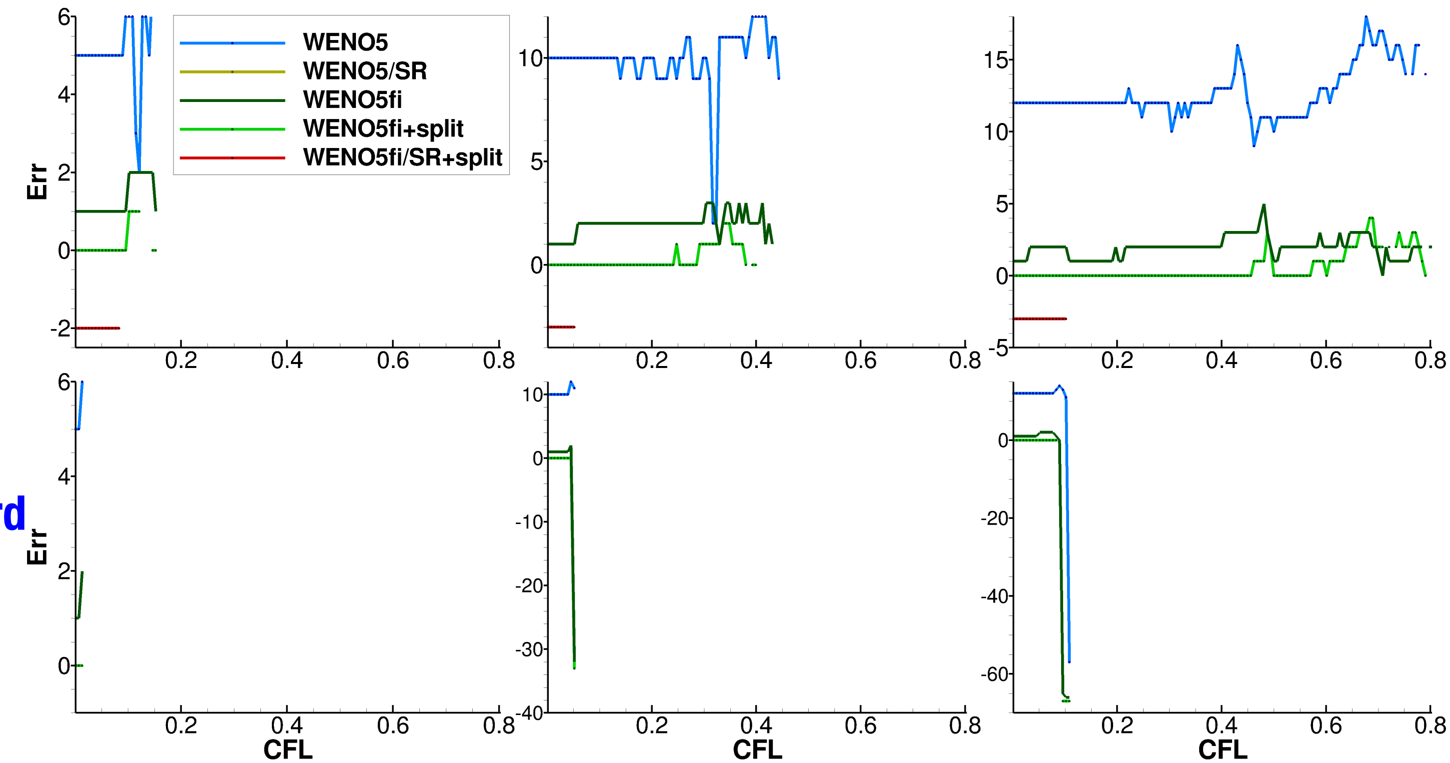

Err: # grid pts. away from exact shock locations

Note: Among the 4 improved schemes WENO5/SR & WENO5fi+split exhibit the least spurious behavior as grid increases

Summary

Same spatial & temporal schemes for the convection operator

(1D C-J Detonation, K_0, and 50, 150 & 300 grid points)

(a) Strang/Safeguard, $N_r > 4$

Can extend the valid CFL range & with more complex spurious behavior

(b) Strang/No-Safeguard, $N_r > 4$

Less spurious behavior than Strang/Safeguard

(c) No-Strang/Safeguard *(Small CFL)*

(d) No-Strang/no-safeguard *(Small CFL; similar to (c))*

General:

> (b) - (d) exhibit a similar CFL range with less spurious behavior than (a).

> No-Strang splitting + Safeguard or No-Safeguard procedures are constrained by a similar CFL range.

> Over all, WENO5/SR & WENO5fi+split in certain cases can improve the results in terms of reducing spurious numerics.

Introduction

NASA Electric Arc Shock Tube (EAST) setup

- Chamber: **10 cm** × **8.5 m**, window at **7 m**
- Shock velocity: **9 – 16 km/sec**
- Gas: $\mathbf{N_2 + O_2}$ driven by **He**
- Pressure after discharge: **1 – 27 atm**
- Driven gas initial pressure: **0.1 – 760 Torr**

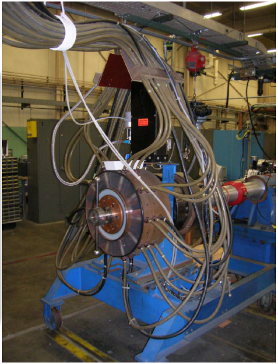

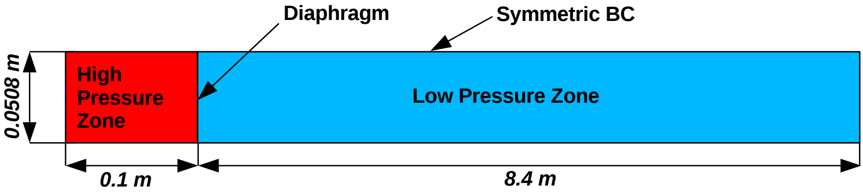

Some CFD Simulation Challenges

- **Small Δt & Δx due to high temperature, viscous BL & stiff chemical reactions**
- **Large computational domain due to long shock tube**

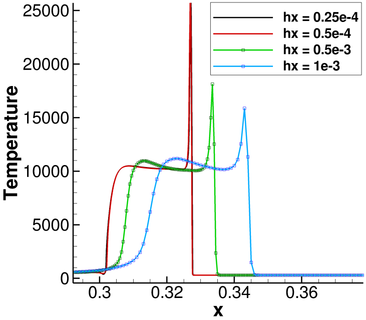

1D Computation, 13 species(Air+He)
4 grid levels:

- $\Delta x = 10^{-3}$
- $\Delta x = 5 \times 10^{-4}$
- $\Delta x = 5 \times 10^{-5}$
- $\Delta x = 2.5 \times 10^{-5}$

Method Comparison

$t_{end} = 3.25 \cdot 10^{-5} sec$, *grid* **600**

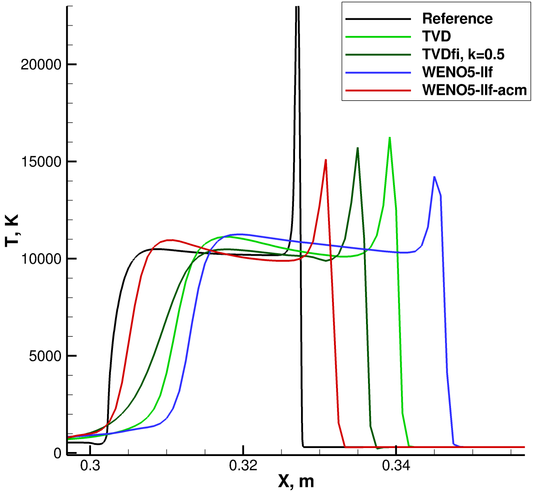

Note: filter version of the schemes gives more accurate solution because of better num. dissipation control

EAST: Temperature Computed at t = 1.e-5 s

Shock/Shear Locations Grid Dependance

TVD, CFL = 0.7

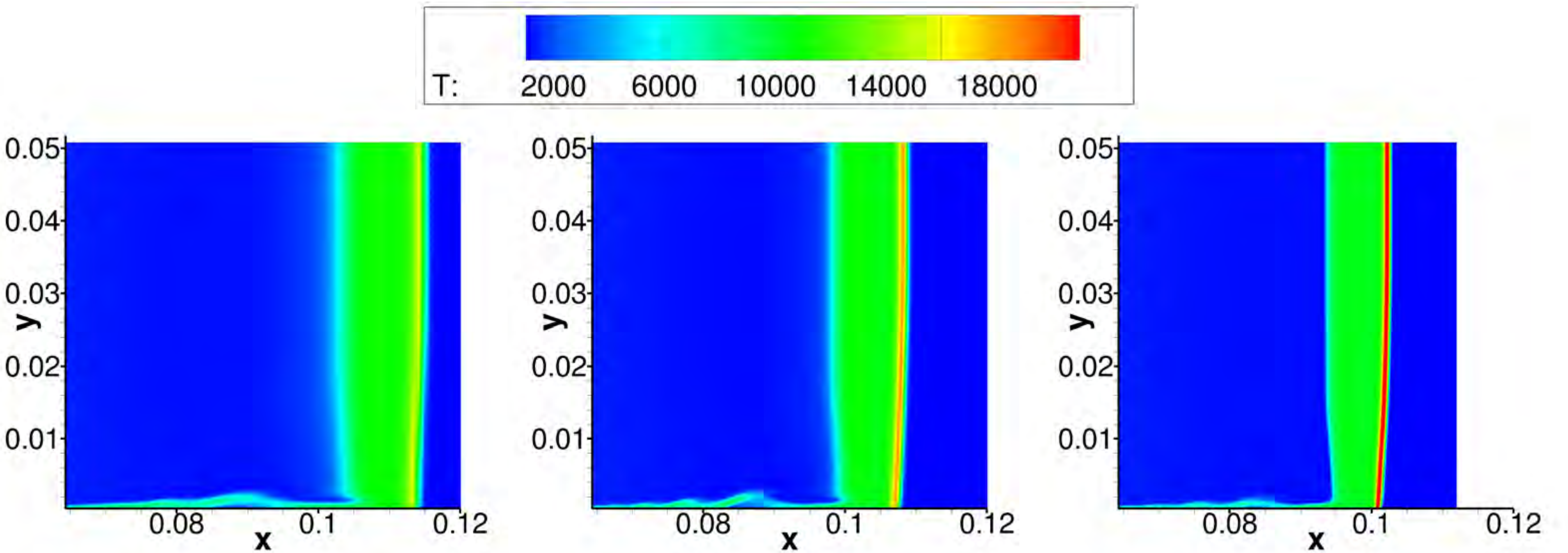

601x121	1201x121	690x121
Uniform in x	Uniform in x	Cluster near shock in x
Tmax = 15,800 K	Tmax = 18,800 K	Tmax = 21,700 K

Fine grid *h* = 0.05 *mm*
Grid points needed for x-dimension: 170,000

Method Comparison

$t_{end} = 10^{-5} sec$, *grid* 691×121, *cluster in X*, $\Delta Y_{min} = 10^{-5}$

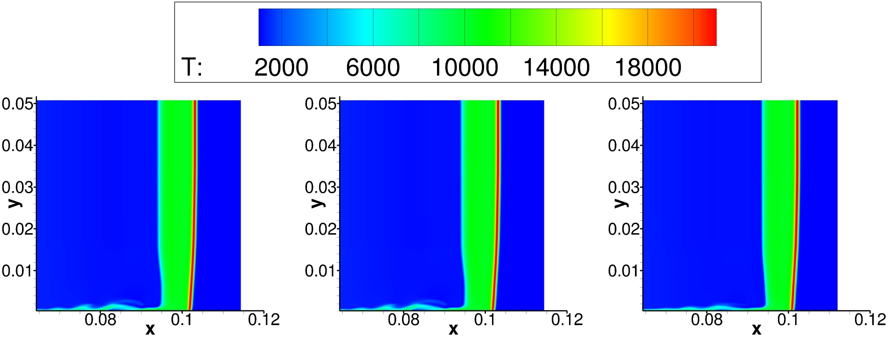

WENO5-LLF
CFL=0.2

WENO5P-LLF
CFL=0.4

TVD
CFL=0.7

Note 1: *Different shock location:* $X_{TVD} = 0.1024\ m$ & $X_{WENO} = 0.1034\ m$

Note 2: *Different boundary layer: Different methods*

Spurious Numerics Due to Source Terms

Source Terms: Hyperbolic conservation laws with source terms – Balanced Law

> *Most high order shock-capturing schemes are not well-balanced schemes*
> *High order WENO/Roe & their nonlinear filter counterparts are well-balanced for certain reacting flows – Wang et al. JCP papers (2010, 2011)*

Stiff Source Terms:

> *Numerical dissipation can result in wrong propagation speed of discontinuities for under-resolved grids if the source term is stiff (LeVeque & Yee, 1990)*

> *This numerical issue has attracted much attention in the literature – last 20 years (Improvement can be obtained for a single reaction case)*

> *A New Sub-Cell Resolution Method has been developed for stiff systems on coarse mesh (Wang et al., JCP, 2012)*

Nonlinear Source Terms:

> *Occurrence of spurious steady-state & discrete standing-wave numerical solutions -- due to fixed grid spacings & time steps (Yee & Sweby, Yee et al., Griffiths et al., Lafon & Yee, 1990 – 2002)*

Stiff Nonlinear Source Terms with Discontinuities:

> *More Complex Spurious Behavior*
> *Numerical combustion, certain terms in turbulence modeling & reacting flows*

Concluding Remarks & Future Plans

- **Studies show the danger in practical simulations for the subject flow without better knowledge of scheme behavior**

  Added Issues not addressed:
  Pointwise evaluation of source terms, Roe average state & ODE solvers

- **Containment of numerical dissipation on schemes can delay the onset of wrong propagation speed**

  > ***WENO5/SR performs better than WENO5fi+split & WENO5fi/SR+split***

  > ***For turbulence with strong shocks WENO5fi+split & WENO5fi/SR+split provide better dissipation control for turbulence***

Future Plans

- **Non-pointwise evaluation of source terms**
- **Correct spurious oscillation near discontinuities due to standard Roe average state**
- **Stiff ODE solver with adaptive error control to alleviate temporal stiffness** ***(interfere with the subcell resolution step)***

Note: Spurious numerics due to spatial discretization is more difficult to contain

Scheme Performance (8 Procs.)

1D Detonation Problem (Grid 300, CFL = 0.05, RK4)

	WENO5	WENO5/SR	WENO5fi+split	WENO5fi/SR+split
CPU eff, iterations/sec	630	610	1720	1590
Discontinuity location error (grid points)	10	0	0	-3

2D Detonation Problem (Grid 500x100, CFL = 0.05, RK4)

	WENO5	WENO5/SR	WENO5fi+split	WENO5fi/SR+split
CPU eff, iterations/sec	4.0	3.6	9.5	5.7
Discontinuity location max error (grid points)	4	0	0	-3

Larger number => more efficient

References

- H.C. Yee, D.V. Kotov, Wei Wang, Chi-Wang Shu. 2013 Spurious Behavior of Shock-Capturing Methods by the Fractional Step Approach: Problems Containing Stiff Source Terms and Discontinuities. J. Comp. Phys. 241, 266-291
- H.C. Yee, D.V. Kotov, W.Wang, C.-W. Shu. 2012 On spurious numerics in solving reactive equations. Annual Research Briefs, Center for Turbulence Research, 347-358
- D.V. Kotov, H.C. Yee, M. Panesi, D. Prabhu, A. Wray. 2012 1D and 2D simulations for the NASA Electric Arc Shock Tube experiments. Annual Research Briefs (Center for Turbulence Research), 359-370
- H.C. Yee, D.V. Kotov, W.Wang, C.-W. Shu. 2012 Spurious behavior of shockcapturing methods: Problems containing stiff source terms and discontinuities. In Proceedings of the ICCFD7. The Big Island, Hawaii
- Jacobs, P. A. 1994 Numerical simulation of transient hypervelocity flow in an expansion tube. Computer & Fluids 23, 77-101
- Lani, A., Sjögreen, B., Yee, H. C. & Henshaw, W. D. 2013 Variable high-order multiblock overlapping grid methods for mixed steady and unsteady multiscale viscous flows, part II: Hypersonic nonequilibrium flows. Commun. Comput. Phys. 13, 583-602
- McCorkle, E. & Hassan, H. 2010 Study of radiation in electric arc shock tubes. In 10th
- AIAA/ASME Joint Thermophysics and Heat Transfer Conferencee. Chicago, Illinois
- Panesi, M., Magin, T., Bourdon, A., Bultel, A. & Chazot, O. 2011 Study of electronically excited
- state populations of atoms and molecules predicted by means of a collisional-radiative model for the fire II flight experiment. Journal of Thermophysics and Heat Transfer 25, 361-374
- Petrie-Repar, P. 1997 Numerical simulation of diaphragm rupture. PhD thesis, University of Queensland
- Sjögreen, B. & Yee, H. C. 2009 Variable high order multiblock overlapping grid methods for mixed steady and unsteady multiscale viscous flows. Commun. Comput. Phys. 5, 730-744

Part I: Foundation for our AIAA CFD Paper

1D & 2D Simulations Related to NASA Electric Arc Shock Tube Experiments (EAST)

(Hypersonic Nonequilibrium Flows)

Solving Reactive Governing Equations

(Different Procedures in solving the Governing Eqs. produce different spurious behavior)

Consider two typical procedures:

- **Fully coupled sysytem**
  - Consistent
  - Small time step due to numerical instability
- **Fractional method using the Strang Splitting of the system**
  - Commonly used in combustion for over 30 years
  - Can extend the valid CFL range but exhibits more complex spurious behavior

Note: Strang Splitting is used for EAST computations

Scalar Case Behavior of WENO5 & WENO5/SR below CFL limit

(Obtaining the Correct Discontinuity Speed)

Source term:

$S = K_0(1-u)(u-0.5)u$

$K_0 = 10{,}000$

Strang/Safeguard

Grid 50 | Grid 150 | Grid 300

Stiff. K_0

Stiff. 100 K_0

Stiff. 1000 K_0

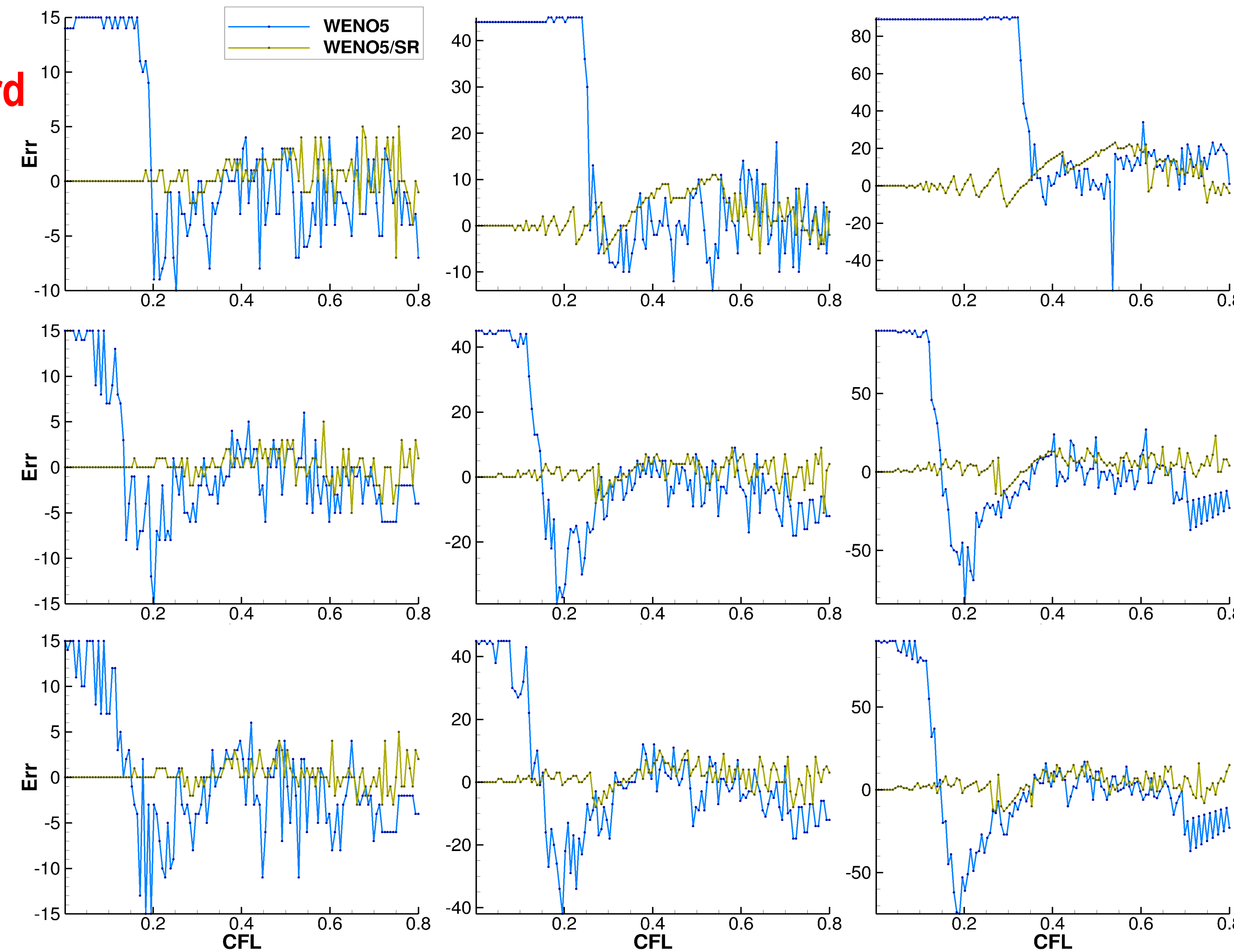

Note: CFL limit based on the convection part of PDE

Behavior of Improved Schemes Below CFL Limit

(Effect of # sub-iteration: Reaction Step Time Integrator, RK1)

1D C-J Detonation

Strang Splitting + Safeguard ODE subiterations

Nr = 1

Nr = 5

Nr = 10

Nr = 100

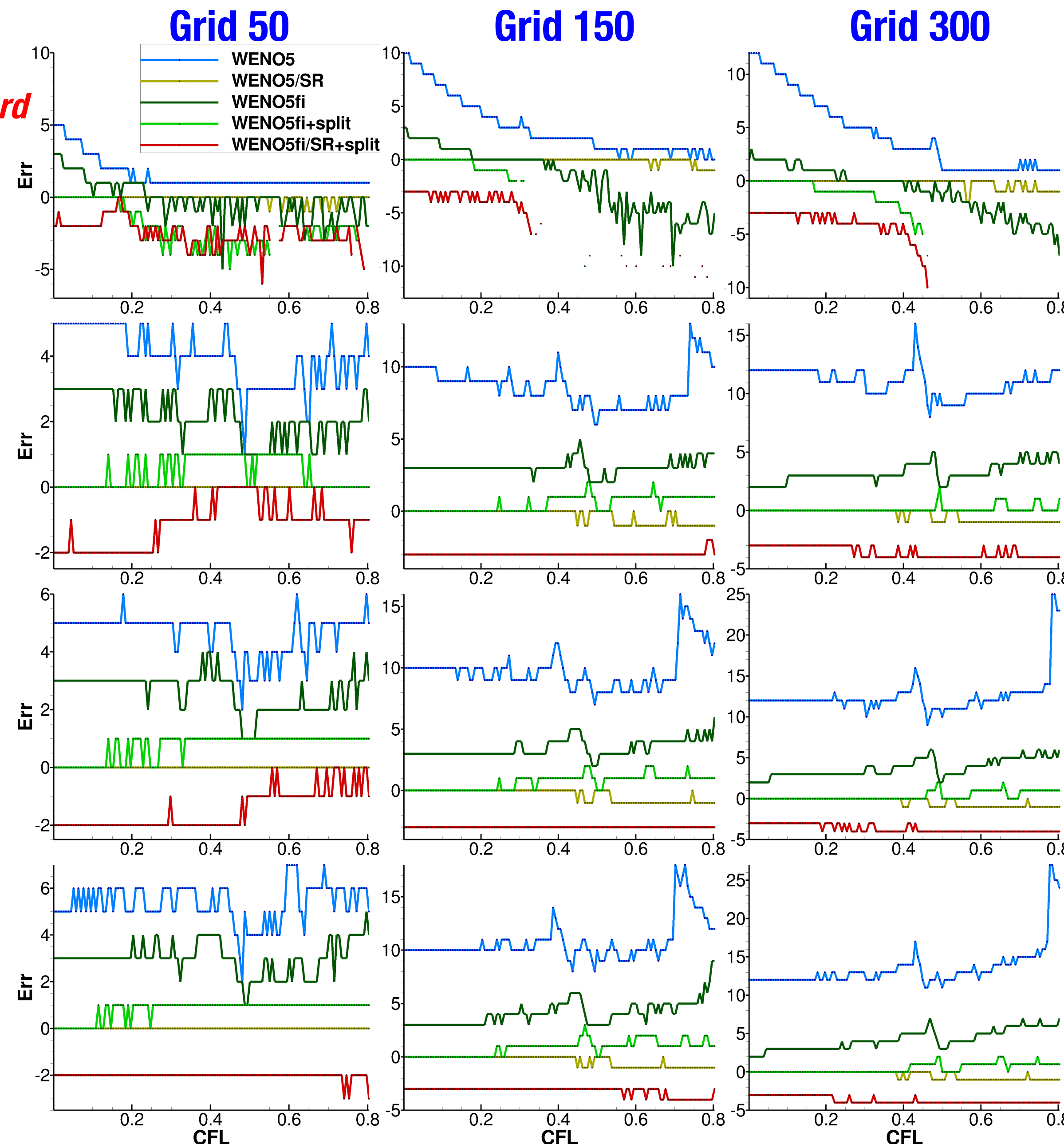

Effort of Different Time Integrator -- Reaction Step

(*Strang Splitting/Safeguard, Nr=4, SR at every RK stage*)

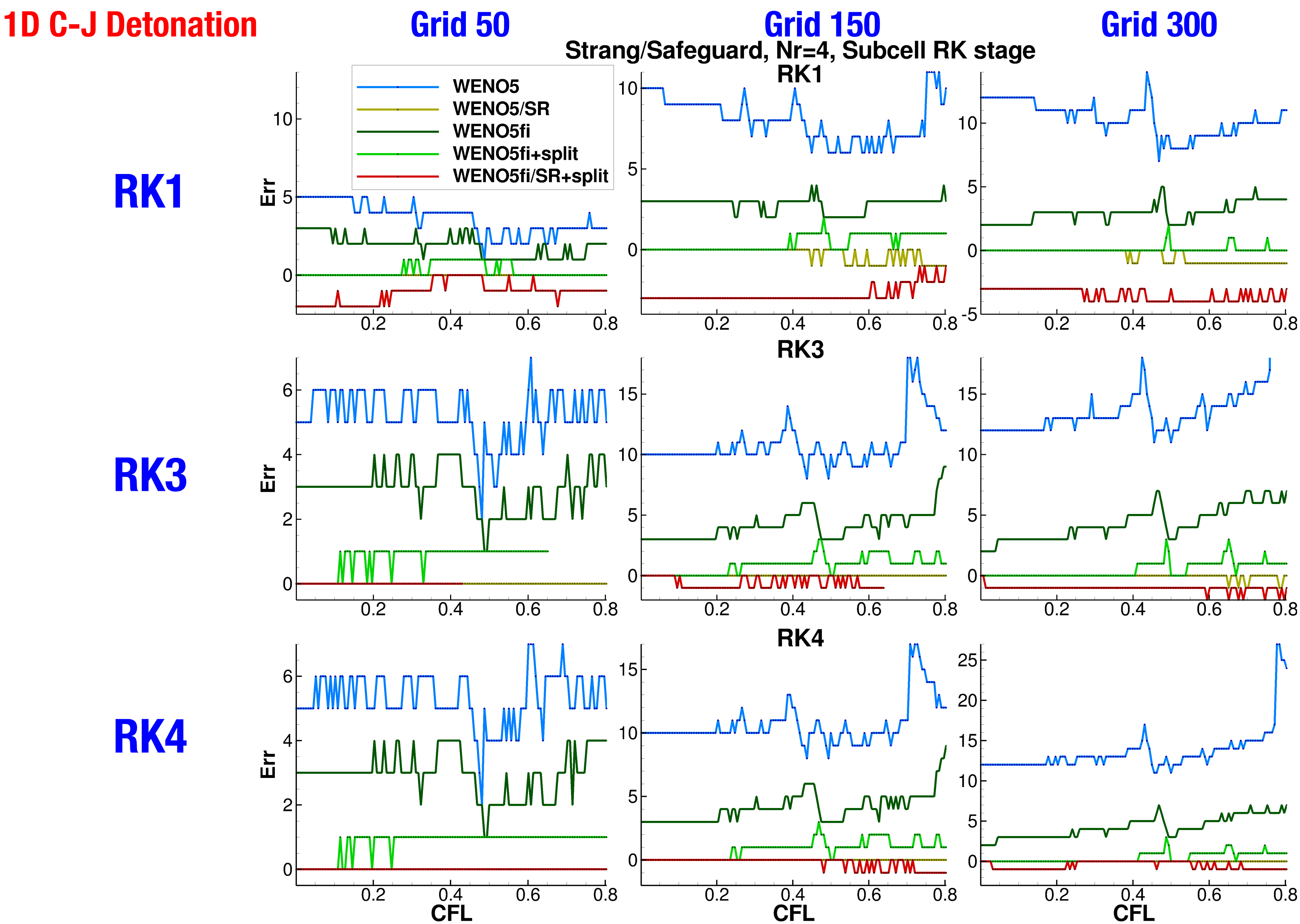

Effort of Different Time Integrator -- Reaction Step

(*Strang Splitting/No-Safeguard, Nr=4, SR at every RK stage*)

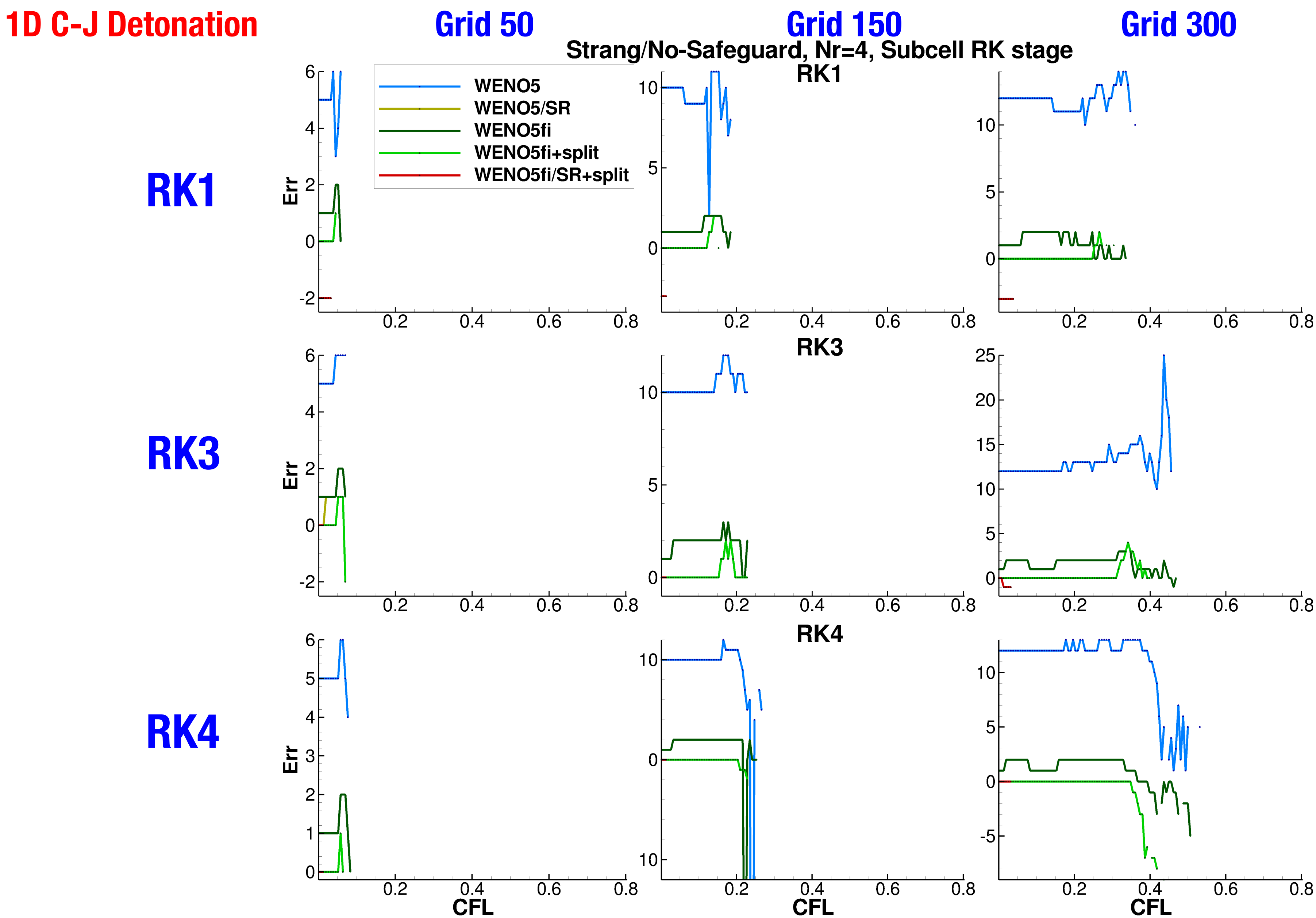

Summary

Same spatial & temporal schemes for the convection operator
(1D C-J Detonation, K_0 , and 50, 150 & 300 grid points)

Explicit Euler (RK1) for the reaction operator:

(a) **Strang/Safeguard**, $N_r > 1$, SR at every subiteration
Can extend the valid CFL range & with more complex spurious behavior

(b) **Strang/No-Safeguard**, $N_r > 1$
Less spurious behavior than Strang/Safeguard

RK2, RK3 & RK4 for the reaction operator:

(a) **Strang/Safeguard**, $N_r > 1$, SR at every subiteration
- *Can extend the valid CFL range & with complex spurious behavior*
- *SR at every RK stage – minor different*

(b) **Strang/No-Safeguard**, $N_r > 1$, SR at every subiteration
- *Less spurious behavior than Strang/Safeguard*
- *No need at every RK stage*

General:
- *Over all, WENO5/SR & WENO5fi+split improve the results in terms of reducing spurious numerics*
- *Higher order RK improve spurious behavior only slightly*

Wrong Propagation Speed of Discontinuities

(WENO5, Two Stiff Coefficients, 50 pts)

1D Detonation

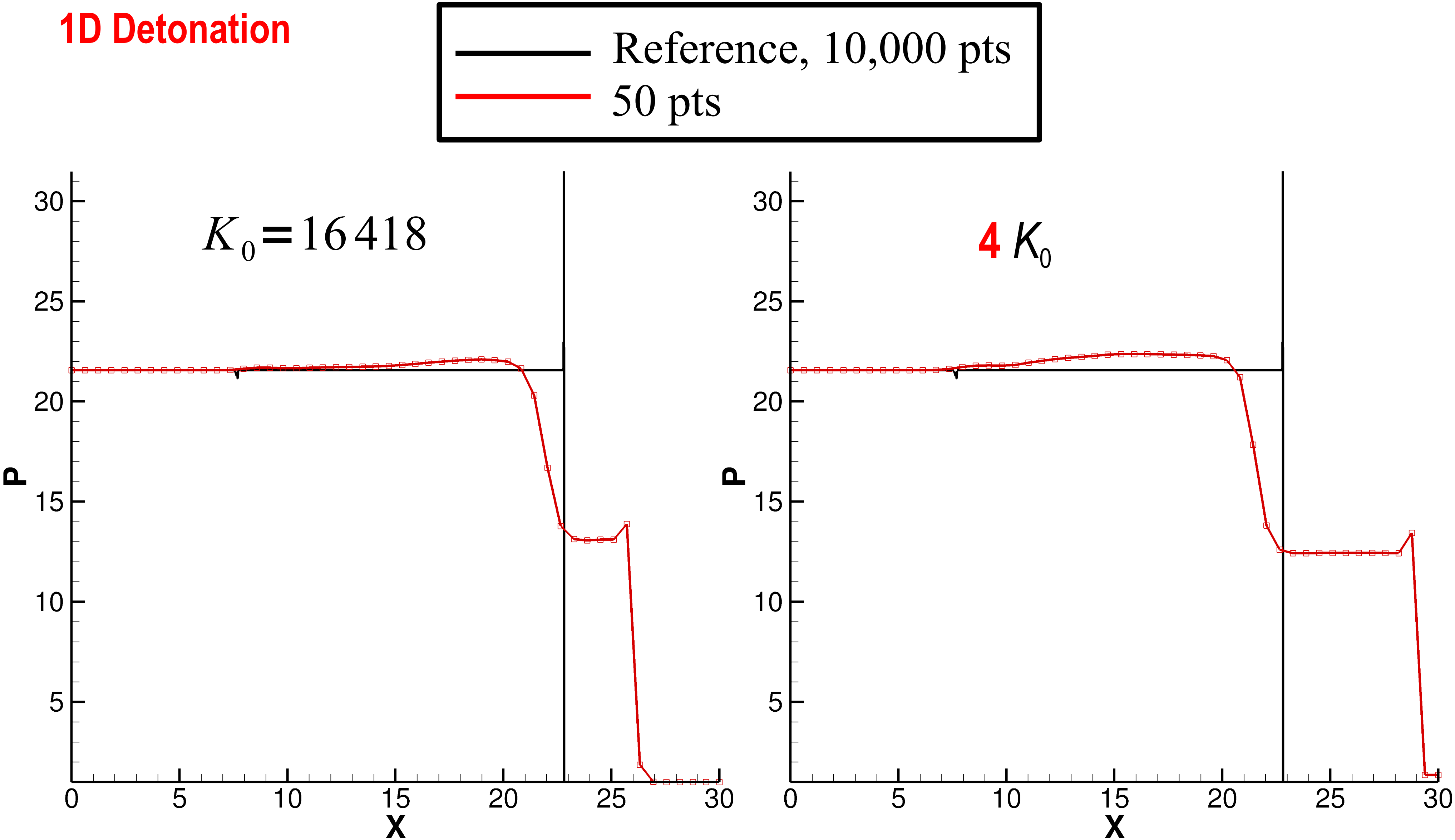

Strang Splitting & Safeguard

Properties of the High-Order Filter Schemes

(Any number of species & reactions)

- High order (4th - 16th) Spatial Base Scheme conservative; no flux limiter or Riemann solver
- Physical viscosity is taken into account by the base scheme (reduce the amount of numerical dissipation to be used if physical viscosity is present)
- Efficiency: One Riemann solve per dimension per time step, independent of time discretizations
- Accuracy: Containment of numerical dissipation via a local wavelet flow sensor
- Well-balanced scheme: Able to exactly preserve certain nontrivial steady-state solutions of the governing equations *(Wang et al. 2011)*
- Parallel Algorithm: Suitable for most current supercomputer architectures

Three Test Cases
(Computed by ADPDIS3D code)

- **1D C-J Detonation Wave**
  (Helzel et al. 1999; Tosatto & Vigevano 2008)

- **2D Detonation Wave** *(Ozone decomposition)*
  (Bao & Jin, 2001)

- **2D EAST Problem (13 species nonequilibrium)**

All schemes employed in the study are included in *ADPDIS3D* solver *(Sjögreen, Yee & collaborators)*

Behavior of Standard Schemes Below CFL Limit

(Different Procedures: TVD, WENO5, WENO7)

1D C-J Detonation

Strang/Safeguard

Strang/No-Safeguard

No-Strang/Safeguard
(Stable for small CFL)

No-Strang/No-Safeguard
(Stable for small CFL)

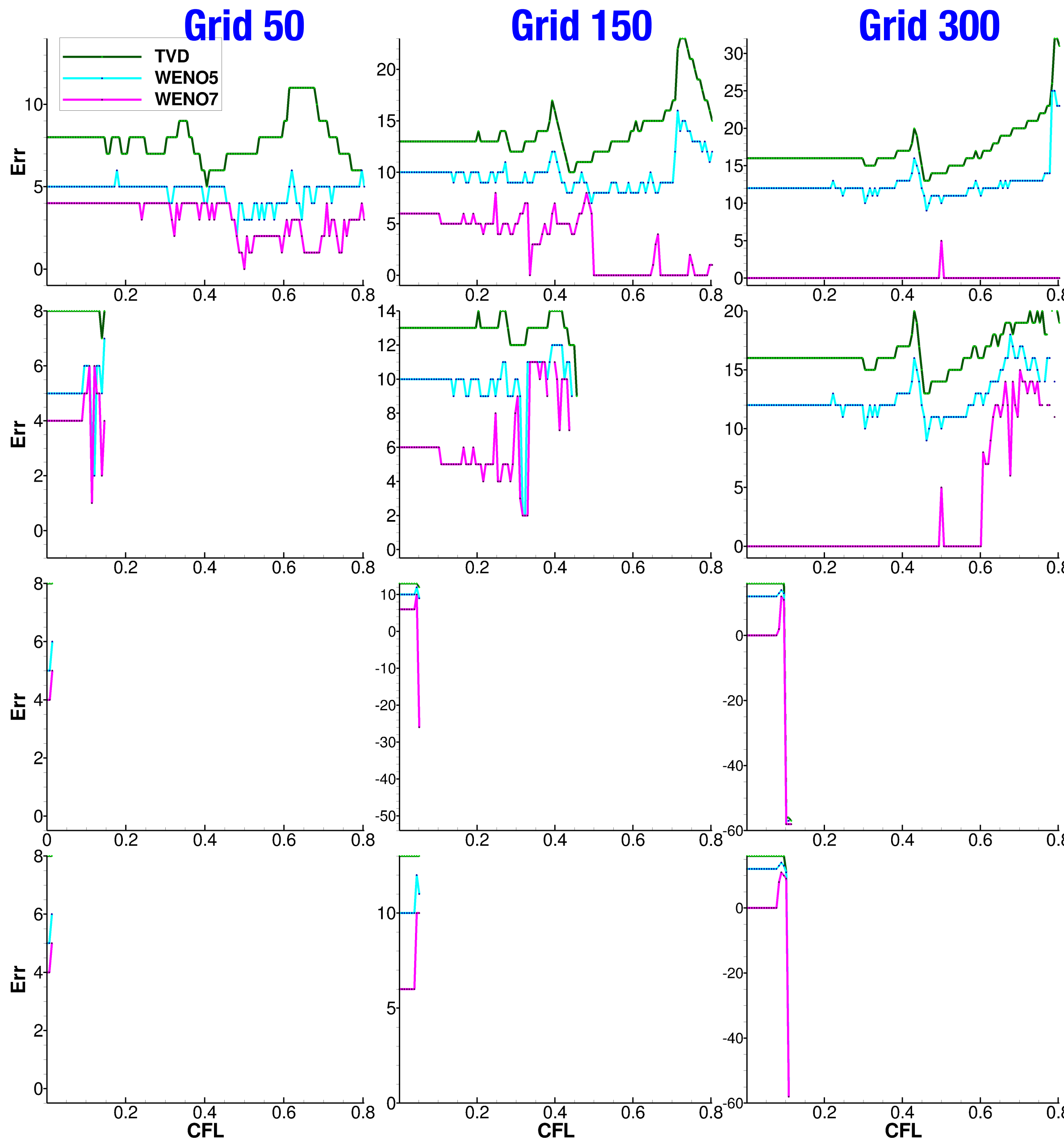

Err: # grid pts.

Behavior of Positivity-Preserving Schemes Below CFL Limit

(Obtaining the Correct Shock Speed)

Strang Splitting, No Safeguard

1D C-J Detonation

Grid 50 | Grid 150 | Grid 300

Hu et al. (WENO5PH)

Zhang & Shu (WENO5P)

WENO5 (Jiang-Shu)

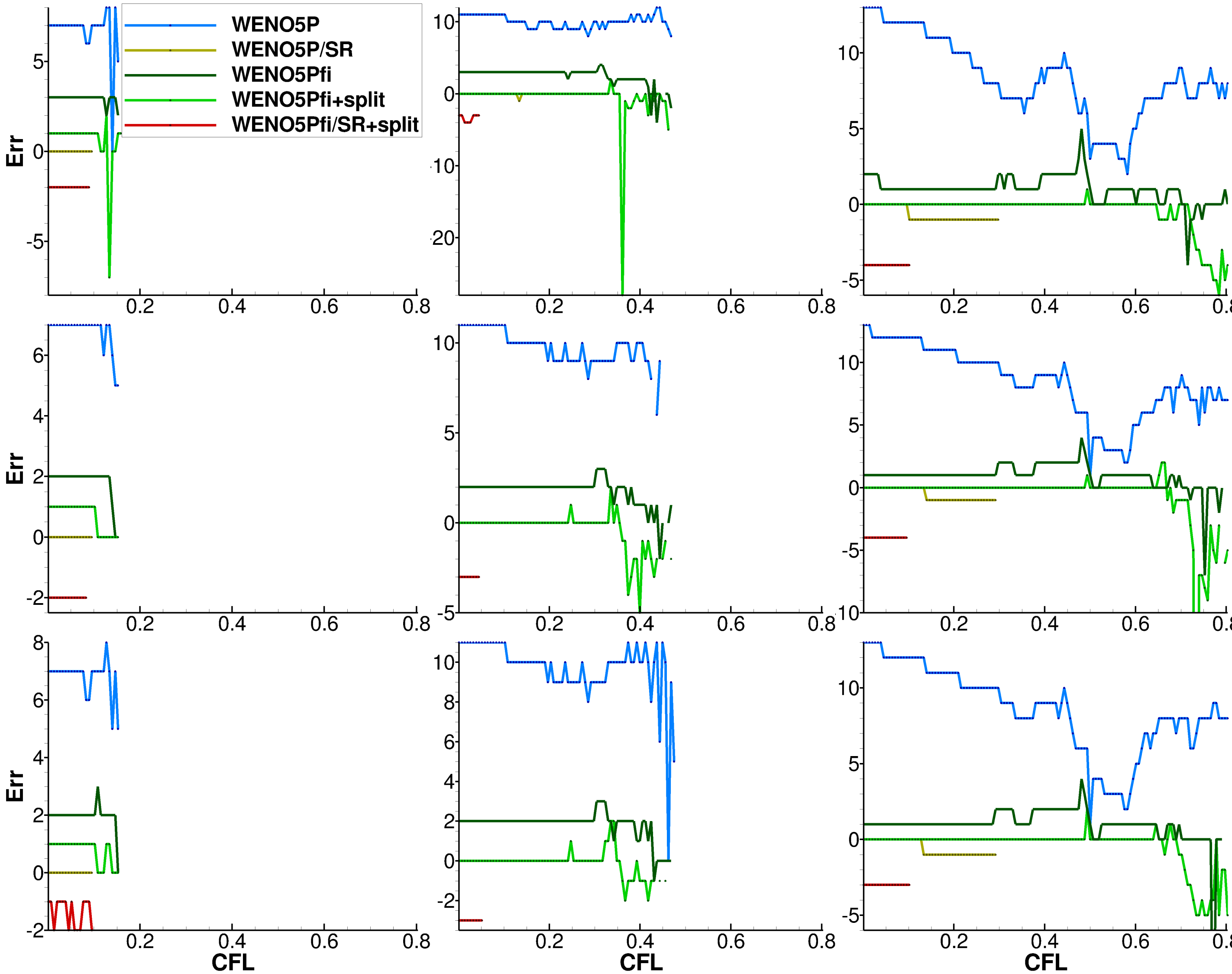

Behavior of Improved Schemes Below CFL Limit

(Different Procedures: Num. Dissip. Control Schemes)

1D C-J Detonation

Strang/Safeguard

Strang/No-Safeguard

No-Strang/Safeguard
(Stable for small CFL)

No-Strang/No-Safeguard
(Stable for small CFL)

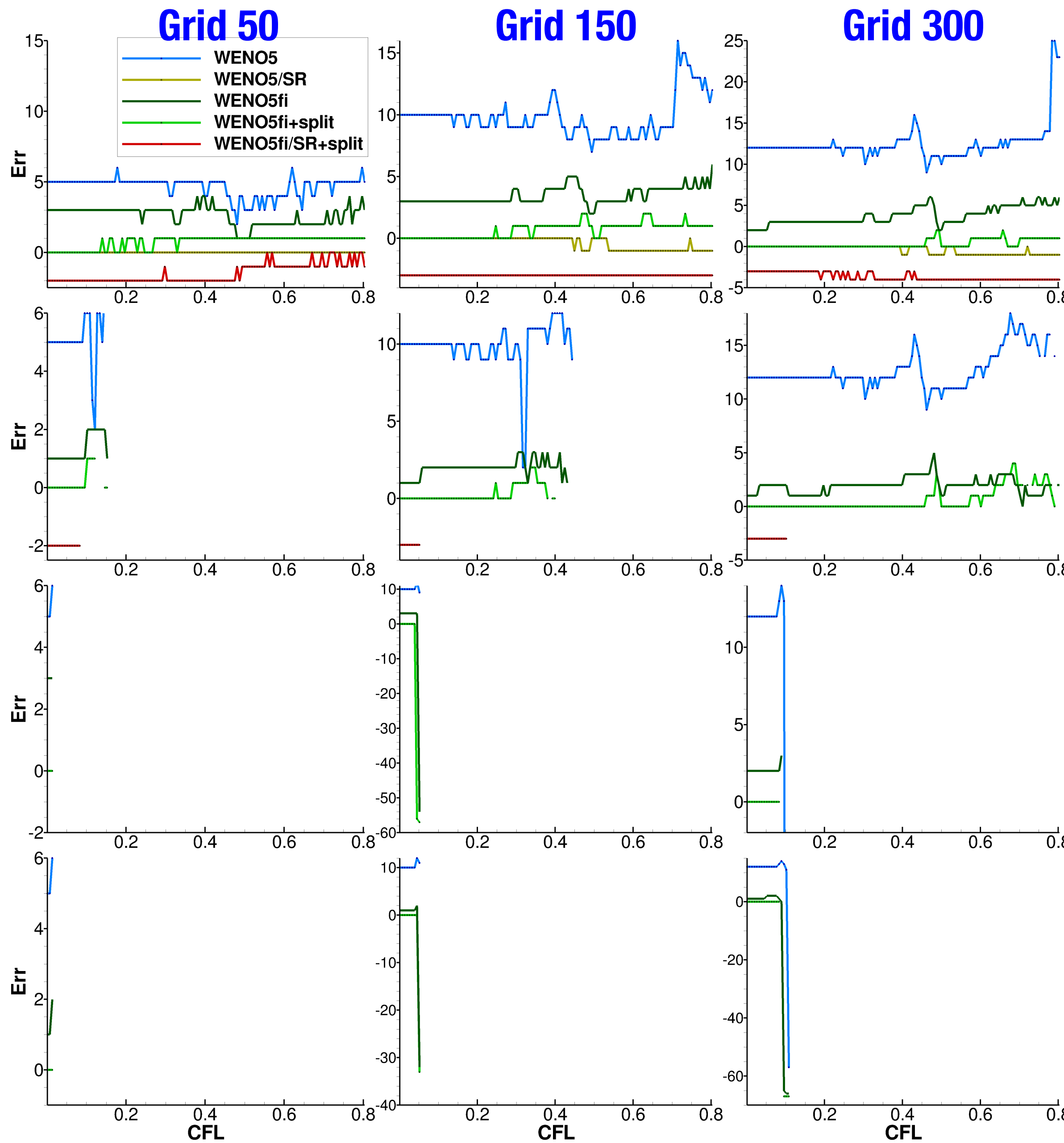

Behavior of Improved Schemes Below CFL Limit

(Effect of # sub-iteration: Reaction Step Time Integrator)

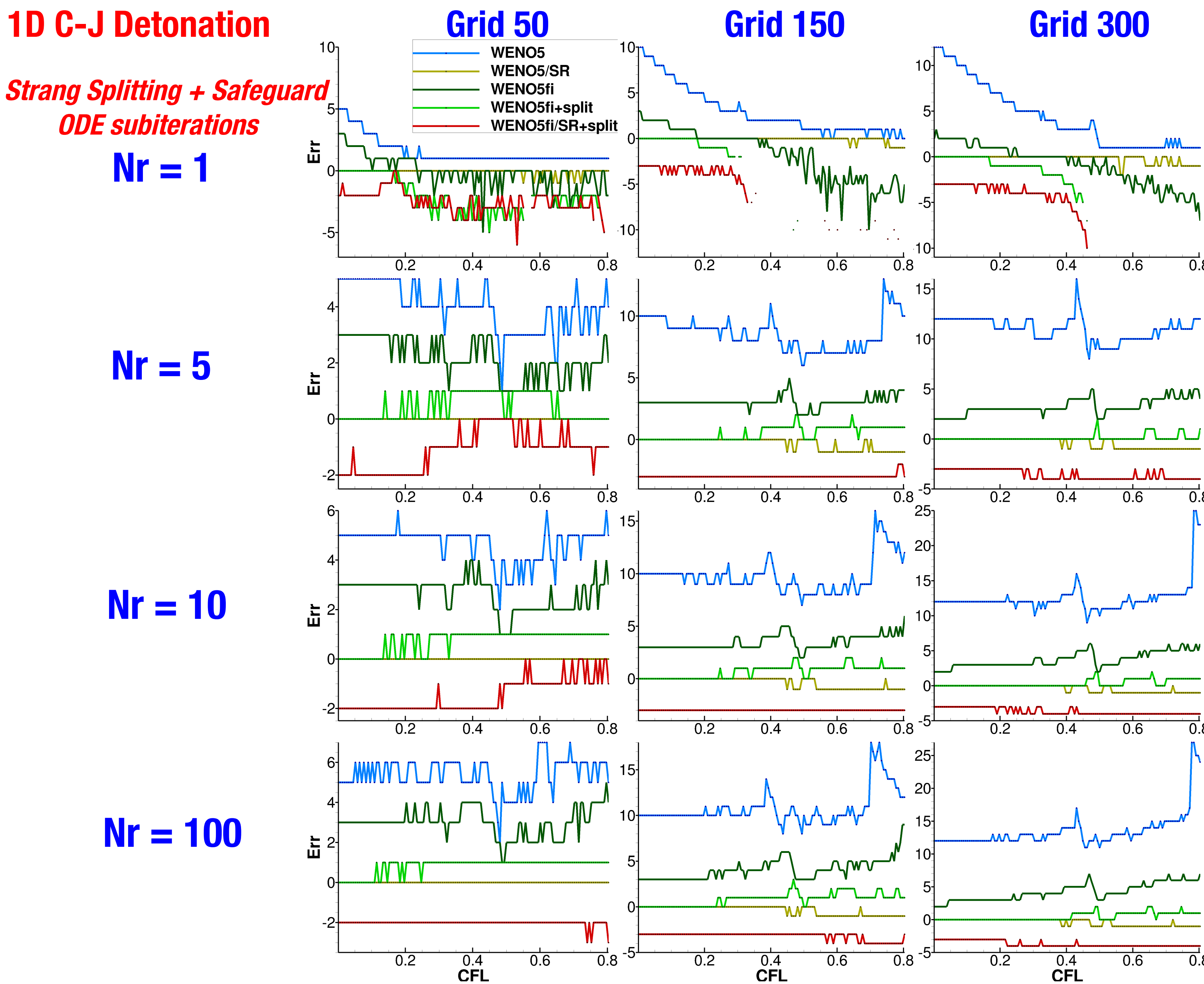

2D Reactive Euler Equations

$$
\begin{aligned}
(\rho_1)_t + (\rho_1 u)_x + (\rho_1 v)_y &= K(T)\rho_2 \\
(\rho_2)_t + (\rho_2 u)_x + (\rho_2 v)_y &= -K(T)\rho_2 \\
(\rho u)_t + (\rho u^2 + p)_x + (\rho u v)_y &= 0 \\
(\rho v)_t + (\rho u v)_x + (\rho v^2 + p)_y &= 0 \\
E_t + (u(E+p))_x + (v(E+p))_y &= 0
\end{aligned}
$$

Unburned gas mass fraction: $z = \rho_2/\rho \qquad \rho = \rho_1 + \rho_2$

Pressure: $p = (\gamma - 1)(E - \frac{1}{2}\rho(u^2 + v^2) - q_0 \rho_2)$

Reaction rate: (a) $K(T) = K_0 \exp\left(\frac{-T_{ign}}{T}\right)$

(b) $K(T) = \begin{cases} K_0 & T \geqslant T_{ign} \\ 0 & T < T_{ign} \end{cases}$

Stiff: large K_0

Reaction Operator

New Approach: Apply Subcell Resolution (Harten 1989; Shu & Osher 1989) to the solution from the convection operator step before the reaction operator

- Identify shock location, e.g. using Harten's indicator for z_{ij} – x-mass fraction of unburned gas:

$$s_{ij}^{x} = minmod\left(z_{i+1,j} - z_{ij}, z_{ij} - z_{i-1,j}\right)$$

Shock present in the cell I_{ij} if

$$\left|s_{i,j}^{x}\right| > \left|s_{i-1,j}^{x}\right| \quad \text{and} \quad \left|s_{i,j}^{x}\right| > \left|s_{i+1,j}^{x}\right|$$

y-direction, similarly:

$$s_{ij}^{y} = minmod\left(z_{i,j+1} - z_{ij}, z_{ij} - z_{i,j+1}\right)$$

- Apply subcell resolution in the direction for which a shock has been detected. If both directions require subcell resolution – choose the largest jump

$$\left|s_{ij}^{x}\right| \quad \text{or} \quad \left|s_{ij}^{y}\right|$$

Reaction Operator *(Cont.)*

For I_{ij} with shock present, $I_{i-q,j}$ and $I_{i+r,j}$ without shock present:

- **Compute ENO interpolation polynomials $P_{i\ q}$ and P_{i+r}**

- **Modify points in the vicinity of the shock (mass fraction z_{ij}, temperature T_{ij} and density ρ_{ij})**

$$\begin{pmatrix} \tilde{z}_{ij} \\ \tilde{T}_{ij} \\ \tilde{\rho}_{ij} \end{pmatrix} = \begin{pmatrix} P_{i-q,j}(x_i, z) \\ P_{i-q,j}(x_i, T) \\ P_{i-q,j}(x_i, \rho) \end{pmatrix}, \quad \theta \geqslant x_i \qquad \begin{pmatrix} \tilde{z}_{ij} \\ \tilde{T}_{ij} \\ \tilde{\rho}_{ij} \end{pmatrix} = \begin{pmatrix} P_{i+r,j}(x_i, z) \\ P_{i+r,j}(x_i, T) \\ P_{i+r,j}(x_i, \rho) \end{pmatrix}, \quad \theta < x_i$$

where Θ is determined by the conservation of energy E:

$$\int_{x_{i-1/2}}^{\theta} P_{i-q,j}(x, E)\,dx + \int_{\theta}^{x_{i+1/2}} P_{i+r,j}(x, E)\,dx = E_{ij}\,\Delta x$$

- **Advance time by modified values for the Reaction operator (use, e.g., explicit Euler)**

$$(\rho z)_{ij}^{n+1} = (\rho z)_{ij}^{n} + \Delta t\, S(\tilde{z}_{ij}, \tilde{T}_{ij}, \tilde{\rho}_{ij})$$

Nonlinear Filter Step $\left(U_t + F_x(U) = 0\right)$

- **Denote the solution by the base scheme (e.g. 6th order central, 4th order RK)**

$$U^* = L^*(U^n)$$

- **Solution by a nonlinear filter step**

$$U_j^{n+1} = U_j^* - \frac{\Delta t}{\Delta x}\left[H_{j+1/2} - H_{j\ \ 1/2}\right]$$
$$H_{j+1/2} = R_{j+1/2}\overline{H}_{j+1/2}$$

$\overline{H}_{j+1/2}$ **- numerical flux,** $R_{j+1/2}$ **- right eigenvector, evaluated at the Roe-type averaged state of** U_j^*

- **Elements of** $\overline{H}_{j+1/2}$ **:**

$$\overline{h}_{j+1/2}^m = \frac{\kappa_{j+1/2}^m}{2}\left(s_{j+1/2}^m\right)\left(\phi_{j+1/2}^m\right) \qquad m = 1\ldots 3 + N_S - 1$$

$\phi_{j+1/2}^m$ **- Dissipative portion of a shock-capturing scheme**

$s_{j+1/2}^m$ **- Wavelet sensor (indicate location where dissipation needed)**

$\kappa_{j+1/2}^m$ **- Control the amount of** $\phi_{j+1/2}^m$

Behavior of standard schemes below CFL limit
(Obtaining the Correct Shock Speed)

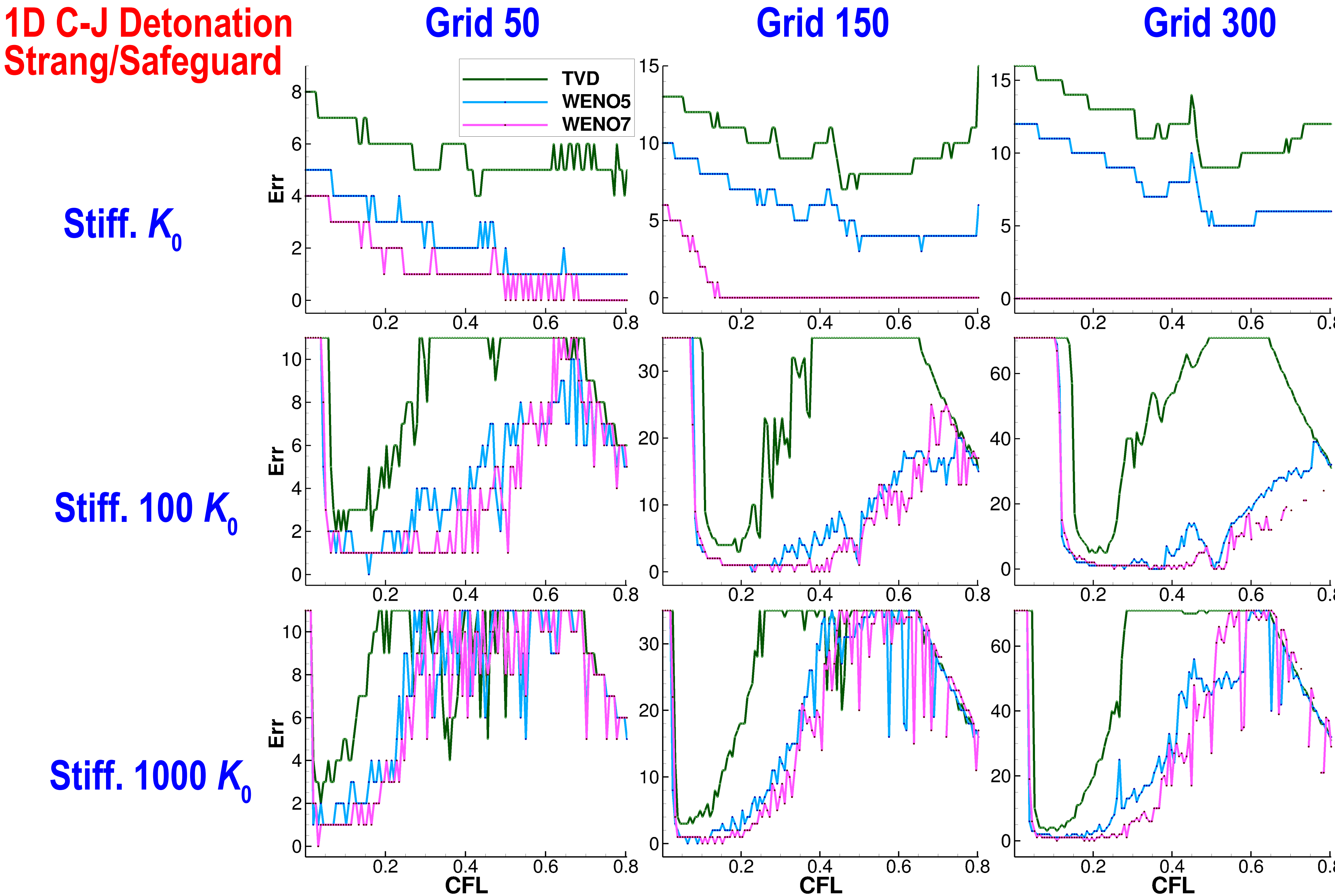

Note: CFL limit based on the convection part of PDEs

Behavior of the schemes below CFL limit

(Obtaining the Correct Shock Speed)

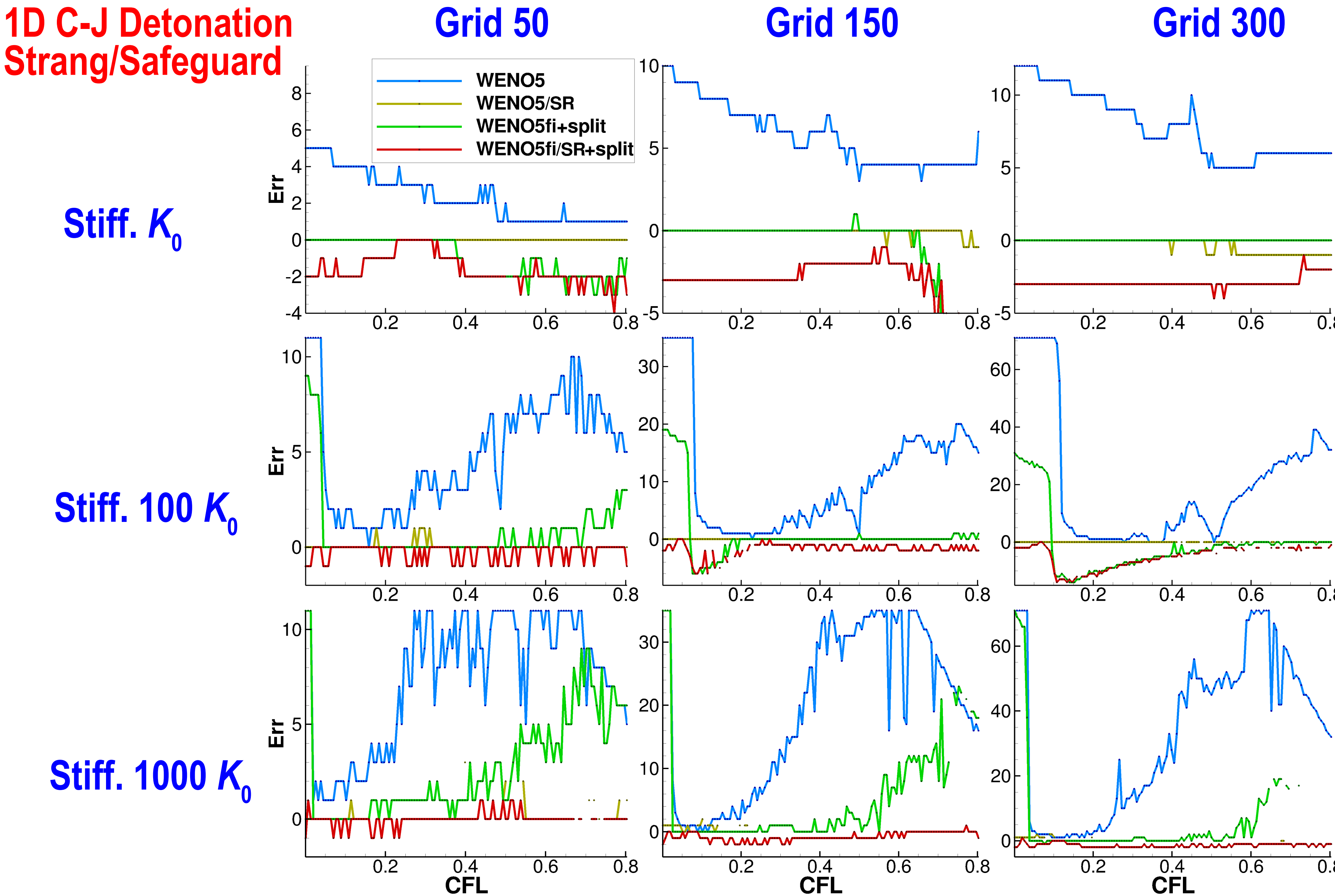

Note: CFL limit based on the convection part of PDEs

2D Detonation Wave

Totally burned gas

$$\begin{pmatrix} \rho_b \\ u_b \\ p_b \end{pmatrix} = \begin{pmatrix} \rho_u \dfrac{[p_b(\gamma+1)-p_u]}{\gamma p_b} \\ 8.162\cdot 10^4 \\ -b+(b^2-c)^{1/2} \end{pmatrix}$$

Totally unburned gas

$$\begin{pmatrix} \rho_u \\ u_u \\ p_u \end{pmatrix} = \begin{pmatrix} 1.201\cdot 10^{-3} \\ 0 \\ 8.321\cdot 10^5 \end{pmatrix}$$

$$S_{CJ} = [\rho_u u_u + (\gamma p_b \rho_b)^{1/2}]/\rho_u$$

$$b = -p_u - \rho_u q_0(\gamma-1) \qquad c = p_u^2 + 2(\gamma-1) p_u \rho_u q_0 / (\gamma+1)$$

Ignition temperature $T_{ign} = 0.1155\cdot 10^{10}$

Heat release $q_0 = 0.5196\cdot 10^{10}$

Rate parameter $K_0 = 0.5825\cdot 10^{10}$

$$K(T) = \begin{cases} K_0 & T \geqslant T_{ign} \\ 0 & T < T_{ign} \end{cases}$$

2D Detonation Wave *(Bao & Jin, 2001)*

Initial Condition

$$\begin{pmatrix} \rho \\ u \\ v \\ p \\ z \end{pmatrix} = \begin{pmatrix} \rho_b \\ u_b \\ 0 \\ p_b \\ 0 \end{pmatrix}, \quad \text{if } x \leqslant \xi(y) \qquad \begin{pmatrix} \rho \\ u \\ v \\ p \\ z \end{pmatrix} = \begin{pmatrix} \rho_u \\ u_u \\ 0 \\ p_u \\ 0 \end{pmatrix}, \quad \text{if } x > \xi(y)$$

$$\xi(y) = \begin{cases} 0.004 & |y - 0.0025| \geqslant 0.001 \\ 0.005 - |y - 0.0025| & |y - 0.0025| < 0.001 \end{cases}$$

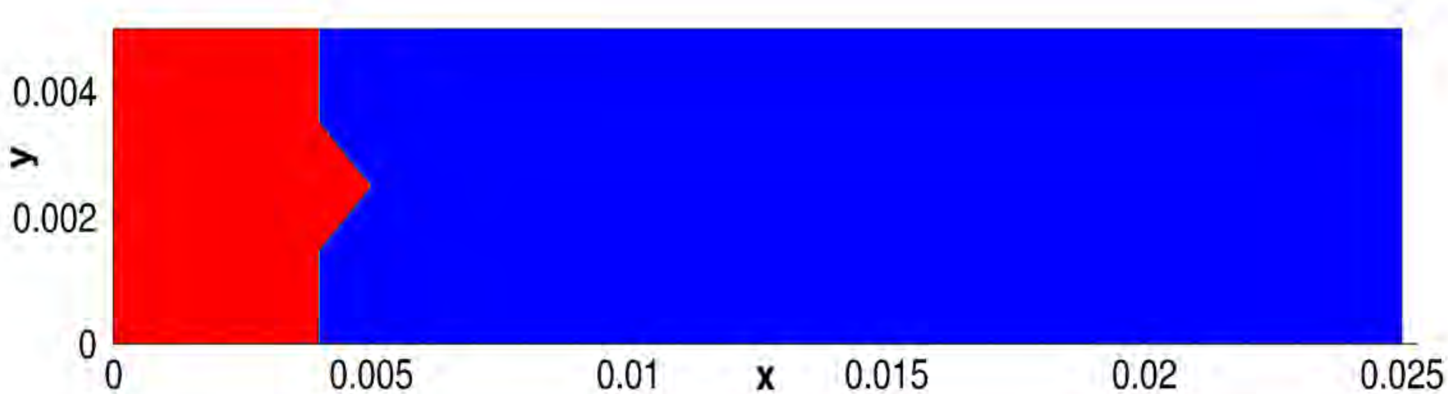

2D Detonation, t=3e-8 s (500x100 pts)

Comparison (WENO5,WENO5/SR,WENO5fi+split)

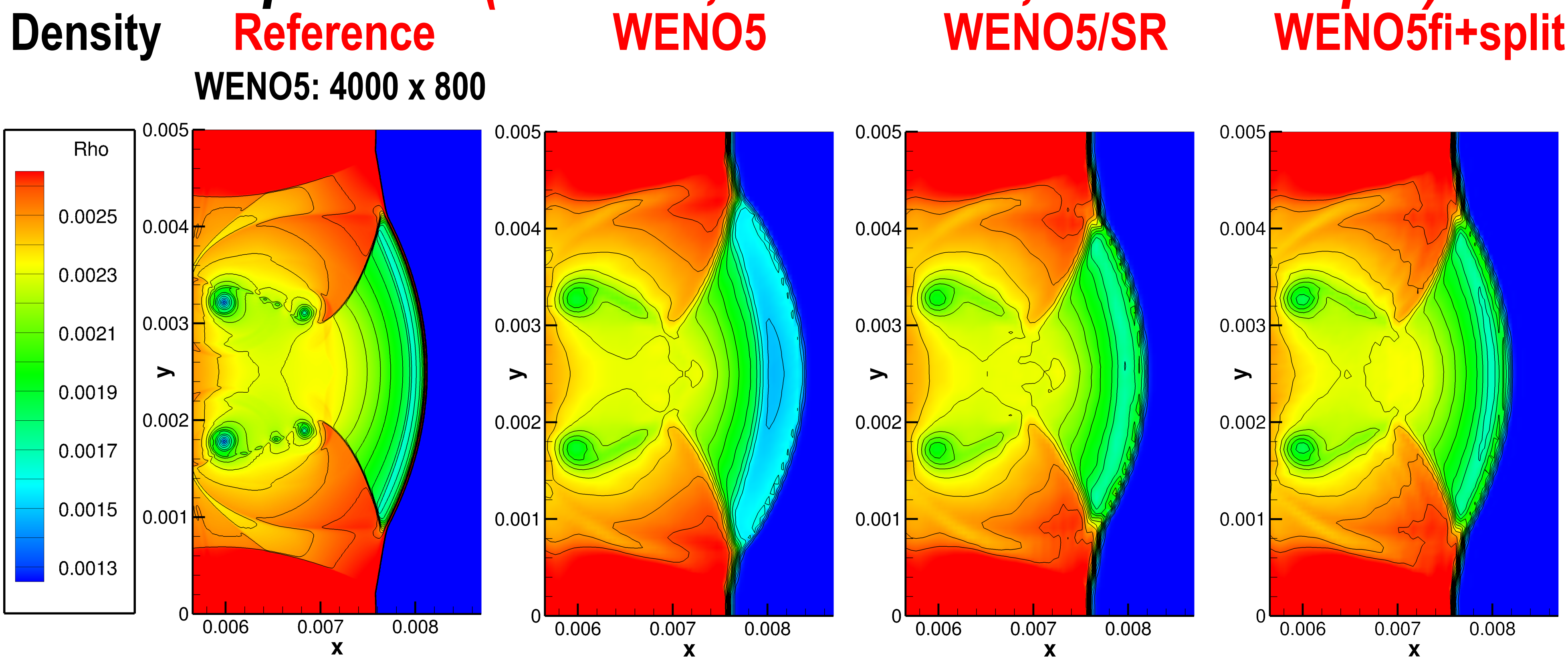

Strang Splitting & Safeguard

2D Detonation, 500x100 pts

WENO5,WENO5/SR,WENO5fi,WENO5fi+split

1D Cross-Section of Density at t = 1.7E-7

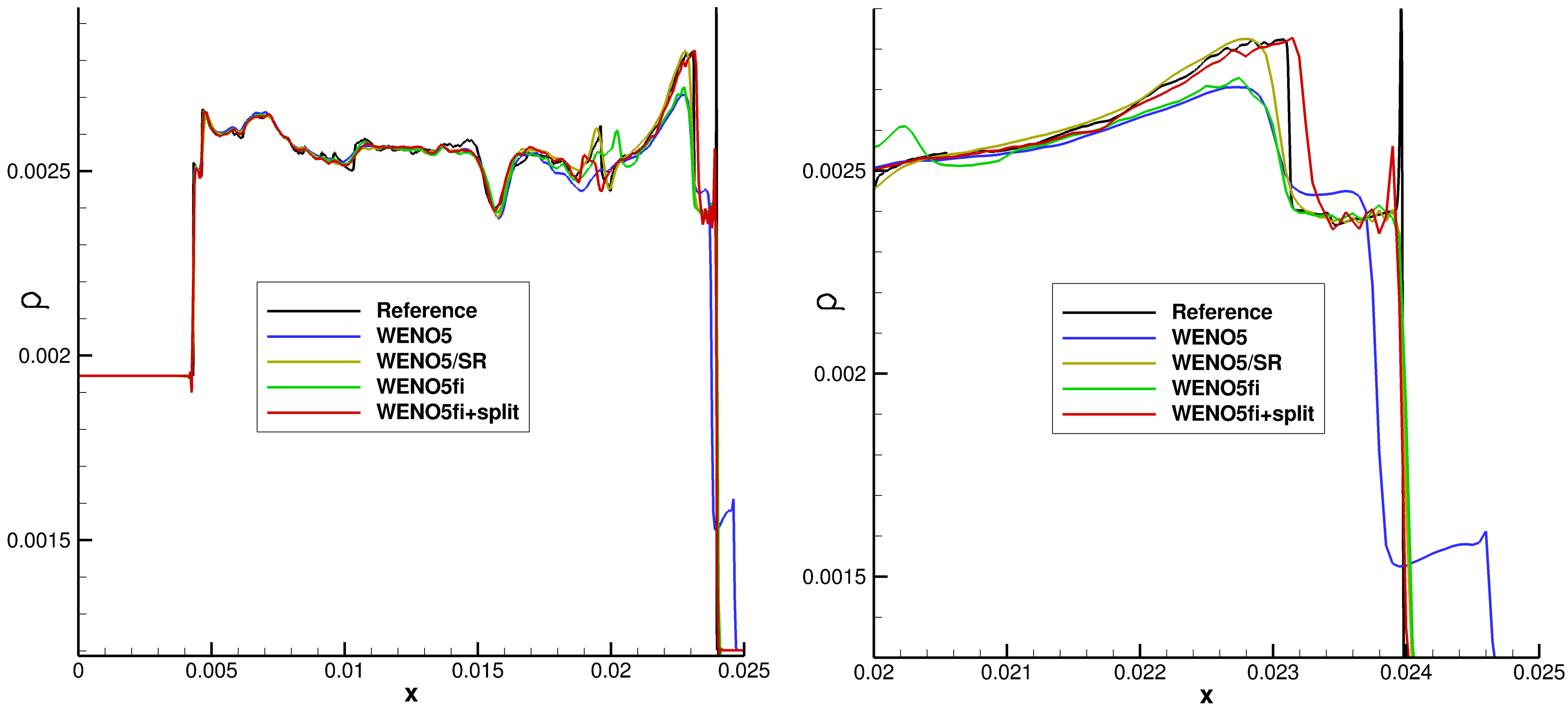

Zoom

Strang Splitting & Safeguard

Note: Wrong shock speed by WENO5fi using 200x40 pts

Behavior of the schemes below CFL limit

(Obtaining the Correct Shock Speed)

2D Detonation

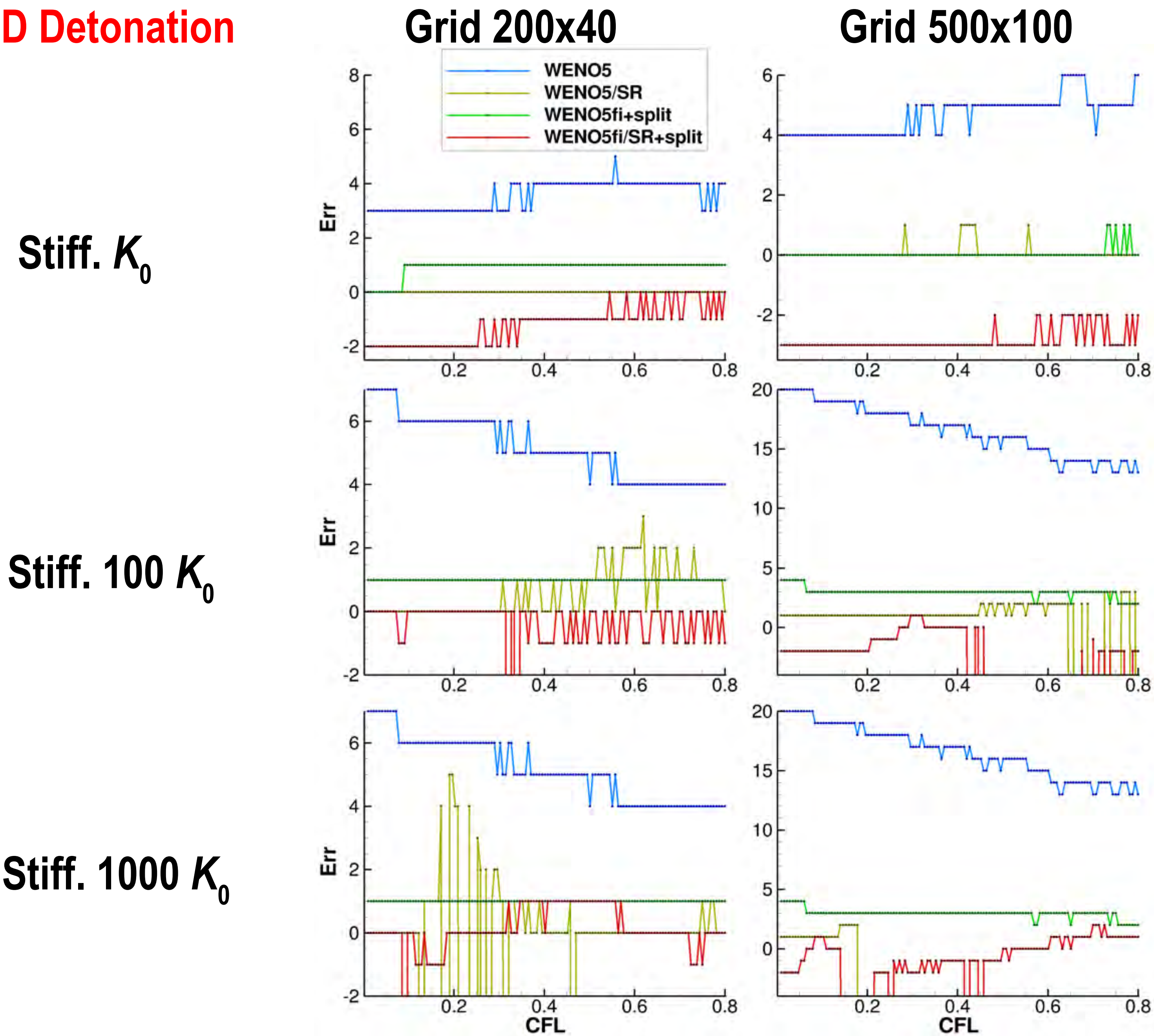

Note: CFL limit based on the convection part of PDEs

EAST Problem. Governing equations

NS equations for 2D (i=1,2) or 3D (i=1,2,3) chemically non-equilibrium flow:

$$\frac{\partial \rho_s}{\partial t}+\frac{\partial}{\partial x_j}(\rho_s u_j+\rho_s d_{sj}) = \Omega_s$$

$$\frac{\partial}{\partial t}(\rho u_i)+\frac{\partial}{\partial x_j}(\rho u_i u_j+p\delta_{ij}-\tau_{ij}) = 0$$

$$\frac{\partial}{\partial t}(\rho E)+\frac{\partial}{\partial x_j}\left(u_j(E+p)+q_j+\sum_s \rho_s d_{sj} h_s-u_i\tau_{ij}\right) = 0$$

$$\rho=\sum_s \rho_s \qquad p=RT\sum_{s=1}^{N_s}\frac{\rho_s}{M_s} \qquad \rho E=\sum_{s=1}^{N_s}\rho_s\left(e_s(T)+h_s^0\right)+\frac{1}{2}\rho v^2$$

$$\tau_{ij}=\mu\left(\frac{\partial u_i}{\partial x_j}+\frac{\partial u_j}{\partial x_i}\right)-\mu\frac{2}{3}\frac{\partial u_k}{\partial x_k}\delta_{ij} \qquad d_{sj}=-D_s\frac{\partial X_s}{\partial x_j} \qquad q_j=-\lambda\frac{\partial T}{\partial x_j}$$

$$\Omega_s=M_s\sum_{r=1}^{N_r}\left(b_{s,r}-a_{s,r}\right)\left[k_{f,r}\prod_{m=1}^{N_s}\left(\frac{\rho_m}{M_m}\right)^{a_{m,r}}-k_{b,r}\prod_{m=1}^{N_s}\left(\frac{\rho_m}{M_m}\right)^{b_{m,r}}\right]$$

Goal

Ultimate Goal

Estimate key flow stuctures by numerical simulation which are of interest for the EAST experiments

Current Goal

Gain first-hand understanding of the computational challenges

- Perform simplified 1D & 2D computations related to NASA EAST experiments
- Illustrate the phenomena that **the discontinuity locations depend on grid spacing & numerical method**

Motivation

(E.g., Grid & method dependence of shock & shear locations)

NASA *Electric Arc Shock Tube* (EAST)
- 1D Computation: 13 species(Air+He) using MUTATION library; L = 8.5 m
- Fine grid step h = 0.05mm, 16 times finer than coarse grid

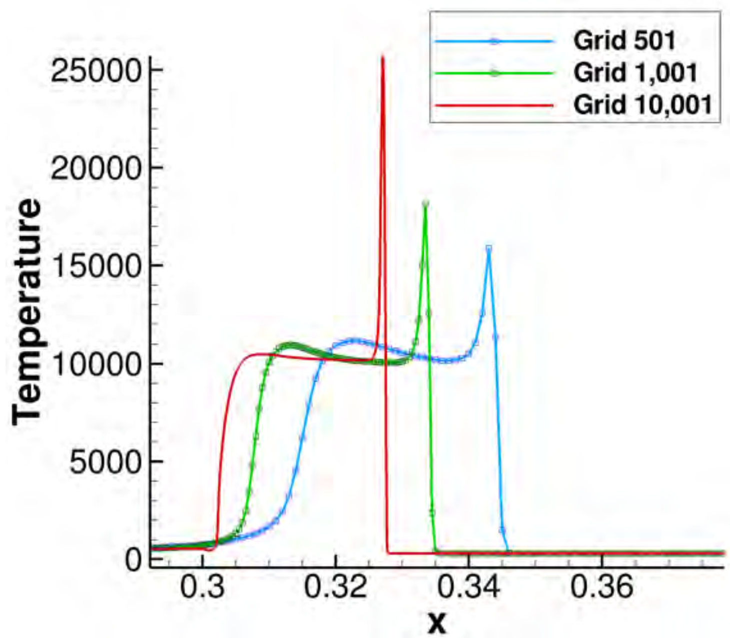

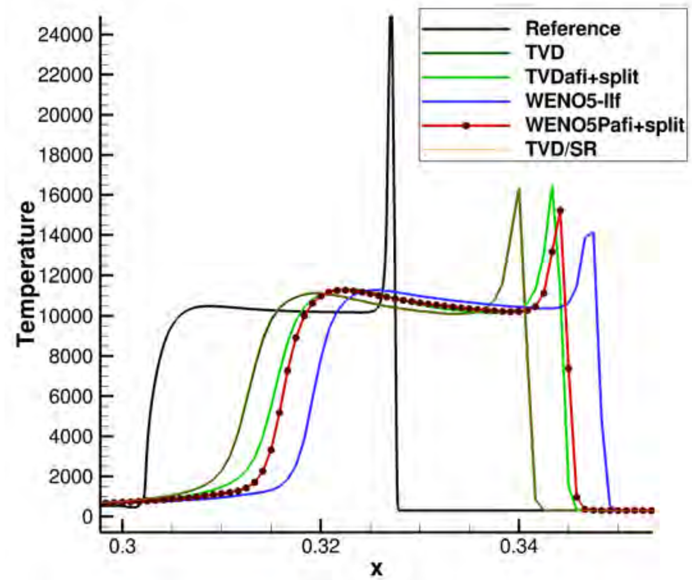

Note: *Non-reacting flows - Grid & scheme do not affect locations of discontinuities, only accuracy*

Implication: *The danger in practical numerical simulation for this type of flow (Non-standard behavior of non-reacting flows)*

2D EAST Problem (Viscous Nonequilibrium Flow)

NASA Electric Arc Shock Tube (EAST) – joint work with Panesi, Wray, Prabhu

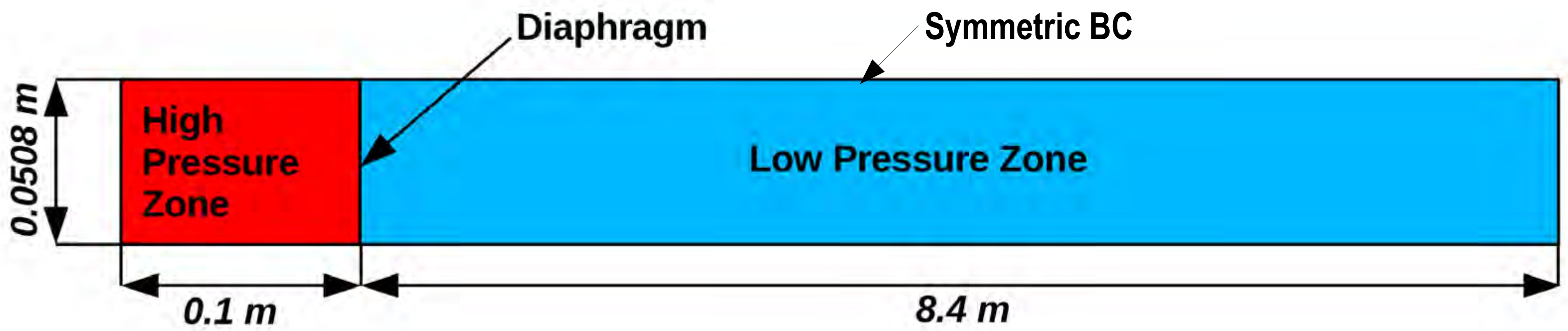

13 Species mixture:

$$e^-, He, N, O, N_2, NO, O_2, N_2^+, NO^+, N^+, O_2^+, O^+, He^+$$

High Pressure Zone

ρ	$1.10546\, kg/m^3$
T	$6000\, K$
p	$12.7116\, MPa$
Y_{He}	0.9856
Y_{N_2}	0.0144

Low Pressure Zone

ρ	$3.0964\text{e}-4\, kg/m^3$
T	$300\, K$
p	$26.771\, Pa$
Y_{O_2}	0.21
Y_{N_2}	0.79

Discontinuity Location Grid Dependence

$TVD, CFL = 0.7, t_{end} = 10^{-5} sec$

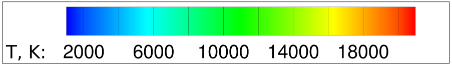

Uniform in X | *Uniform in X* | *Cluster in X*

Stretch in Y:
$\Delta Y_{min} = 10^{-5} m$

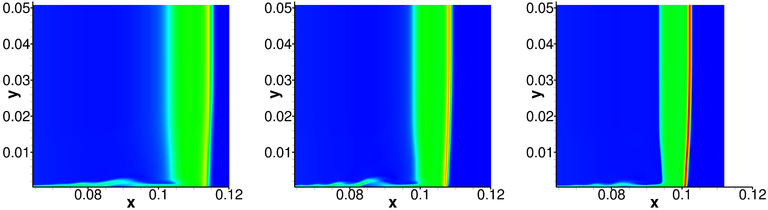

601×121 | 1201×121 | 691×121

Stretch in Y:
$\Delta Y_{min} = 0.5 \cdot 10^{-5} m$

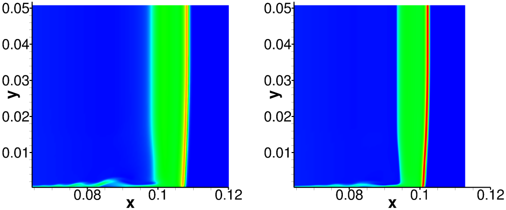

1201×121 | 691×121

Note: Distance between shear & shock depends on Δx & scheme